CHARACTERIZATION OF THE EXTRACELLULAR MATRIX PRODUCED BY HUMAN BONE MARROW MESENCHYMAL STEM CELLS UNDERGOING OSTEOGENIC DIFFERENTIATION ON CHITOSAN/GELATIN SCAFFOLDS

MASTER THESIS

FOTIOS PAPADOGIANNIS

DEPARTMENT OF MATERIALS SCIENCE AND TECHNOLOGY

UNIVERSITY OF CRETE, HERAKLION GREECE

OCTOBER 2018

Supervisor: Prof. Maria Chatzinikolaidou

Co-supervisors: Prof. Maria Vamvakaki, Prof. Charalampos Pontikoglou

ACKNOWLEDGMENTS

This thesis was performed from September 2017 until October 2018 in collaboration with the Laboratory for Hematology at the Faculty of Medicine.

I would like to thank all those who supported me during this work. First, a big thank to my supervisors, Professor Maria Chatzinikolaidou and Professor Charalampos Pontikoglou who motivated me with their knowledge in Biology and Medicine to deal with biomaterials and tissue engineering and perform my Bachelor and Master thesis. A big thank also to Professor Maria Vamvakaki for her continuous support since my Bachelor studies.

Also, many thanks deserve to the Post-Doc researcher Aristea Batsali whose educational skills were very valuable to me. She taught me to think scientifically, and the right way to work in a laboratory.

Also, all members of the Haemopoiesis Research Lab, Professor Helen Papadaki, Mrs Irene Mavroudi, Mrs Athina Damianaki, Ms Semeli Mastrodimou, Mrs Rena Fragkiadaki who contributed in many positive ways.

I would also like to thank Dr. Anthie Georgopoulou and all the members of the Biomaterials Laboratory for the excellent collaboration and their valuable help.

Many thanks to all members of the Chemical Engineering Lab in Imperial College London where I performed a 5-month Erasmus Internship and especially Professor Athanasios Mantalaris and Dr Michail Klontzas. They inspired me, and I gained a lot of experience from them as they taught me many new and interesting techniques.

Finally, I would like to thank Olina, my family and my friends who supported me when I faced difficulties and encouraged me in every educational and scientific step.

CONTENTS

ABSTRACT

In the present study we aim at extending our previous observations on the osteogenesis supporting capacity of 40:60% chitosan/gelatin (CS/Gel) scaffolds, by evaluating the composition of extracellular matrix (ECM) produced by human bone marrow mesenchymal stem cells (BM-MSCs) undergoing osteogenic differentiation on these scaffolds. BM-MSCs were characterized based on their morphologic/immunophenotypic characteristics and their osteogenic/adipogenic differentiation potential. BM-MSCs were cultured on the scaffolds or on tissue culture polystyrene (TCPS) controls and induced towards osteocytes. The scaffolds' osteogenic promoting capacity was demonstrated by the mRNA expression of the osteogenic markers RUNX2, ALP, OSC, DLX5. Notably, ALP and OSC mRNA expression was higher in the scaffolds compared to TCPS. A PCR array was used to assess the mRNA expression of 29 bone ECM-associated genes. We demonstrate, for the first time, the differential expression of 28/29 genes within the CS/Gel scaffolds compared to TCPS. Genes encoded for collagens type I A1 and type V A1, ECM protease inhibitors and osteopontin, among others, were significantly downregulated in the scaffolds, whereas genes encoding for ECM proteases and vitronectin were upregulated. Immunofluorescence data for the detection of the bone ECM proteins collagen type I A1, and osteopontin were in line with the PCR array results. In conclusion, we have provided a comprehensive characterization of bone ECM in cultures of human BM-MSCs differentiated towards osteocytes in CS/Gel scaffolds. Our findings are anticipated to contribute to better understanding of the complex cell-scaffold interactions within the matrix microenvironment, and are of importance for bone tissue engineering applications.

INTRODUCTION

Fundamentals of Bone Biology

The human skeleton is a highly dynamic organ, which is composed of more than 200 bones in adulthood (1, 2). Bones perform a wide array functions and respond to a variety of metabolic, physical and endocrine stimuli. Bones represent the foundation for our bodily locomotion, provide load-bearing capacity to our skeleton and protection to our internal organs, house the biological elements required for haemopoiesis, trap dangerous metals (i.e., lead) and maintain the homeostasis of key electrolytes via calcium and phosphate ion storage. In addition, bone is engaged in a constant cycle of resorption and renewal, undergoing continual chemical exchange and structural remodeling (1, 2).

Bones are composed of four different types of cells embedded in a mineralized extracellular matrix i.e. the osteoblasts, the osteoclasts, the osteocytes and the lining cells (2).

The osteoblasts are cuboidal cells that are responsible for bone formation (2, 3). They derive from mesenchymal stem/stromal cells (MSCs) through the timely activation of the Wingless-int (Wnt) pathway and the synthesis of Bone Morphogenetic proteins (BMPs) along with the expression of Runt related transcription factor 2 (Runx2; a master gene of osteogenesis), Distal-less homeobox 5 (Dlx5) and the osterix (Osx) (2, 4, 5). Once a pool of osteoblast progenitors expressing Runx2 and collagen type I A1 (Col1A1) has been established during osteoblast differentiation, a proliferation phase ensues. At this stage, osteoblast progenitors exhibit alkaline phosphatase activity (ALP) and are characterized as preosteoblasts (2, 4, 5). The transition of preosteoblasts to mature osteoblasts is characterized by an increase in the expression of Osx and in the secretion of bone matrix proteins such as osteocalcin (OCN), bone sialoprotein (BSP) I/II, and collagen type I (2, 4, 5). These proteins along with osteonectin, osteopontin and proteoglycans, including decorin and biglycan form the organic matrix which is subsequently mineralized (2).

Bone lining cells are quiescent flattened osteoblasts that cover bone surfaces (2, 6). Their functions are not entirely understood, however it has been shown that these cells prevent the direct interaction between osteoclasts and bone matrix, so as to avoid bone resorption at sites where the latter should not occur. In addition, bone lining cells participate in osteoclast differentiation, producing osteoprotegerin (OPG) and the receptor activator of nuclear factor kappa-B ligand (RANKL) (2, 6).

Osteocytes, which comprise 90–95% of bone cells are located within lacunae surrounded by mineralized bone matrix, where they show a dendritic morphology (2, 7, 8). They derive from MSCs through osteoblast terminal differentiation. In this process, four recognizable stages have been proposed: osteoid-osteocyte, preosteocyte, young osteocyte, and mature osteocyte (2, 7, 8). During osteoblast/osteocyte transition and before osteocytes are embedded within the bone matrix, cytoplasmic processes start to emerge. These cytoplasmic processes are connected to other neighboring osteocytes processes by gap junctions, as well as to cytoplasmic processes of osteoblasts and bone lining cells on the bone surface, facilitating the intercellular transport of small signaling molecules such as prostaglandins and nitric oxide, as well as oxygen and nutrients (2, 7, 8). Once mature osteocytes totally entrapped within mineralized bone matrix are formed, several of the previously expressed osteoblast markers such as OCN, BSPII, collagen type I, and ALP are downregulated. On the other hand, osteocyte markers including dentine matrix protein 1 (DMP1) and sclerostin are highly expressed (2, 7, 8).

Osteoclasts are bone cells responsible for the dissolution and absorption of mineralized bone (2, 9, 10). They are large terminally multinucleated cells formed through fusion of mononuclear precursors under the influence of several factors including the macrophage colony-stimulating factor (M-CSF) and the RANK ligand (RANKL) (2, 9, 10). On the other hand, OPG binds to RANKL and prevents the interaction with its receptor (RANK) on the surface of osteoclast precursors, thereby inhibiting osteoclastogenesis. In this context the RANKL/RANK/OPG system is a key mediator of osteoclastogenesis (2, 9, 10).

The extracellular matrix of the bone

The extracellular matrix (ECM) of the bone is a composite of an organic phase

reinforced by an inorganic phase (2, 11). Bone matrix not only provides mechanical support, but is also actively implicated in bone homeostasis and in the regulation of bone cells, via adhesion molecules, mainly integrins. The organic matrix contains collagenous proteins (90%), predominantly type I collagen, and noncollagenous proteins including OCN, osteonectin, osteopontin, fibronectin and BSPII, BMPs and growth factors (2, 11). ECM contains also small leucine-rich proteoglycans including decorin, biglycan, lumican, osteoaderin, and seric proteins (2, 11). Proteoglycans provide resistance to compressive forces. The inorganic material of bone consists predominantly of phosphate and calcium ions, which nucleate to form the hydroxyapatite crystals ($Ca_{10}(PO_4)_6(OH)_2$). Together with collagen, the noncollagenous matrix proteins form a scaffold for hydroxyapatite deposition and such association is responsible for the typical stiffness and resistance of bone tissue (2, 11).

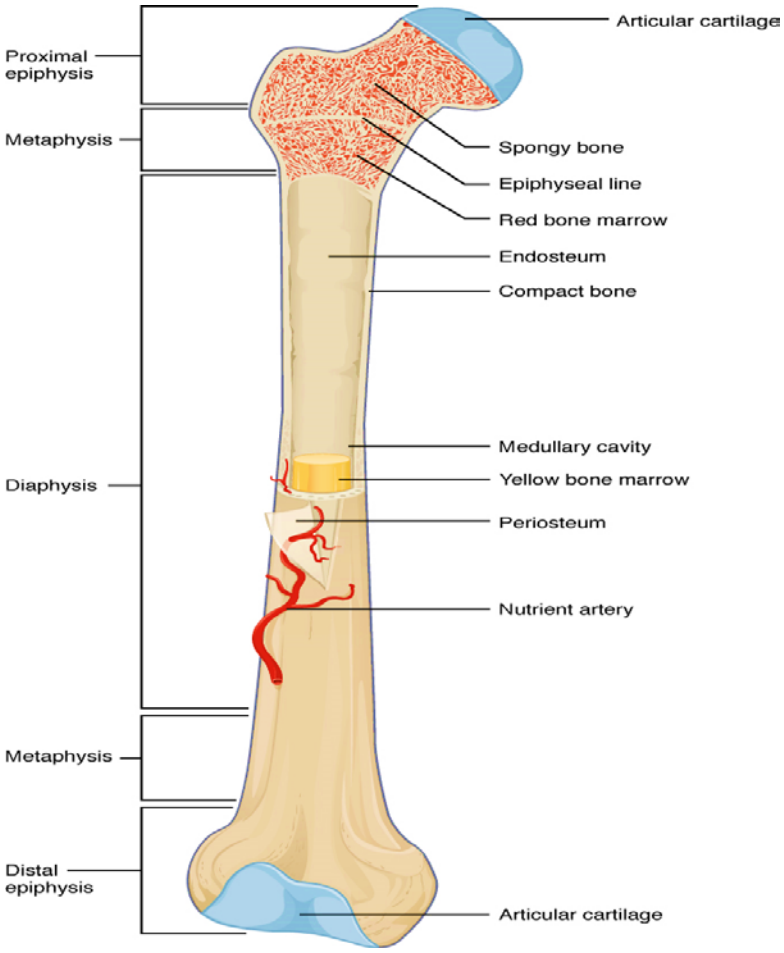

Figure 1. Structure of the Bone

[https://opentextbc.ca/anatomyandphysiology/chapter/6-3-bone-structure/]

Therapeutic approaches of bone defects

Bones can regenerate and repair themselves and thus in most clinical situations, bone injuries and fractures heal without scar formation. Nevertheless, in pathological fractures or large bone defects, bone healing and repair often fail, resulting in delayed unions or non-unions.

Current therapeutic modalities for critical bone injuries include autologous and allogeneic transplantations using autografts and allografts (1). At present, autografts represent the gold standard for bone grafts because they are histocompatible and non-immunogenic and have osteoinductive and osteoconductive properties. However autologous bone transplantation is a very expensive procedure and it may also result in significant donor site injury and morbidity (1). Also, allografts, the second most common bone-grafting technique may be associated with transmission of infections and immune reactions (1).

Bone tissue engineering (BTE) (1) offers a promising alternative strategy of healing severe bone injuries, without the limitations and drawbacks of current therapeutic modalities. The classic BTE paradigm consists of appropriately combining three building blocks: a biocompatible scaffold that closely mimics the bone ECM, bone forming cells and growth factors.

Mesenchymal Stem/Stromal Cells in Bone Tissue Engineering

A source of human cells that can be derived in large numbers from a small and easy initial harvest and can differentiate into bone-forming cells is preferable for cell-based BTE constructs (12). Various cell types have been explored for BTE applications, each with its own potential and premise (13). Among these, MSCs from the bone marrow (BM-MSCs) have been thoroughly investigated in tissue engineering approaches for bone regeneration (12). BM-MSCs are multipotent non-haemopoietic stromal cells that can differentiate into a variety of cell types including osteoblasts, chondrocytes, and adipocytes (14). They are typically isolated from the mononuclear layer of the BM following separation by density gradient centrifugation. The mononuclear cells are subsequently cultured in medium with 10% fetal calf serum, and the MSCs adhere to the bottom of the culture flask showing fibroblast-like morphology (14). Cultured-expanded BM-MSCs typically

express a number of surface receptors including CD29, CD44, CD49a-f, CD51, CD73, CD105, CD106, CD166, and Stro1 and lack expression of definitive hematopoietic lineage markers including CD11b, CD14, and CD45 (14). Similar cells have also been isolated from several other tissues, such as skeletal muscle, adipose tissue, umbilical cord, synovium, dental pulp, amniotic fluid, as well as fetal blood, liver, BM, and lung. However, these populations do not seem to be equivalent in terms of multipotency (14).

The incorporation of BM-MSCs into BTE scaffolds is a widely studied strategy for accelerated bone formation during bone defect repair and regeneration (1, 12). The mechanisms by which enhanced bone regeneration occurs involve direct provision of BM-MSCs for osteogenic differentiation and bone formation, as well as enhanced capacity of the scaffold to promote bone growth via the release of osteogenic growth factors and stimulation of the migration and differentiation of host osteoprogenitors (1). In addition, pre-differentiating MSCs into the osteogenic lineage before implantation has been shown to further accelerate bone repair and osteointegration of the construct *in vivo* by delivering a more mature osteogenic population capable of immediate bone formation (1). Preclinical trials with BM-MSC-seeded constructs have proven effective in accelerating bone repair in various scenarios, including critical-size femoral defects and cranio-maxillofacial deformities (12).

Scaffolds for Bone Tissue Engineering

When designing the appropriate scaffold for BTE one should into consideration several important properties including:

Biocompatibility: This is prerequisite for the adherence, growth, proliferation and migration of bone forming cells on the material surface. Moreover, biocompatibility ensures that following implantation the scaffold will elicit a negligible immune reaction only (1, 15).

Biodegradability: Scaffolds and constructs are not intended as permanent implants. Thus, scaffolds must be biodegradable in order to allow cells to produce their own extracellular matrix. Interestingly, the by-products of this degradation must be non-

toxic and able to be excreted from the body without interference with other organs (1, 16).

Scaffold architecture: The architecture of scaffolds used for tissue engineering is of critical importance (1, 17). Scaffolds should have a properly interconnected pore structure an adequate porosity to ensure cellular penetration and adequate diffusion of nutrients to cells within the construct and to the ECM formed by these cells. Furthermore, a porous interconnected structure is required to allow diffusion of waste products out of the scaffold. The mean pore size plays also a key role in tissue engineering applications (1, 17). Although some ambiguity remains surrounding the optimal pore size for a three-dimensional scaffold, it is generally agreed that pores should be large enough to facilitate cell migration into the structure, where they eventually become bound to the ligands within the scaffold, as the interaction between cells and scaffolds is achieved via chemical groups (ligands) such as Arg-Gly-Asp (RGD) binding sequences. On the other hand pores must be small enough to allow efficient binding of a critical number of cells to the scaffold (1, 17). Therefore, the appropriate pore size depends on the cell type and the tissue being engineered.

Mechanical properties: The mechanical properties of the scaffolds used in tissue engineering applications should match that of the host tissue. Moreover, scaffolds should be strong enough to allow surgical handling during implantation (1).

Historically, first generation biomaterials for bore repair included metals (such as titanium or titanium alloys), synthetic polymers (such as poly(methyl methacrylate), Teflon-type) and ceramics (such as alumina and zirconia) (18). These biomaterials commonly resulted in the formation of fibrous tissue at the biomaterial-tissue interface that would eventually encapsulate the graft, subsequently leading to aseptic loosening. This occurred as a non-specific immune response to a material that cannot be phagocytosed.

To avoid this non-specific immune response, second generation biomaterials were developed by modifying first generation biomaterials with coatings that are bioactive or biodegradable (18). These bone substitute materials include synthetic and naturally-derived biodegradable polymers (*i.e.* collagen, polyesters), calcium phosphates (synthetic or derived from natural materials such as corals, algae, bovine

bone), calcium carbonate (natural or synthetic), calcium sulfates, and bioactive glasses (silica or non-silica based) (18).

Third generation bone graft substitutes include biomaterials capable of inducing specific cellular responses at the molecular level, by integrating the bioactivity and biodegradability of second generation devices (18). This type of bone graft is based on the concept of bone tissue engineering. The latter aims at creating a construct that enhances bone repair and regeneration by incorporating bone progenitor cells and growth factors into a scaffold made of various natural or synthetic biomaterials or their combination and with sufficient vascularization to allow access to nutrients to support this process (18).

Among the major groups of biomaterials used for tissue-engineered scaffold fabrication including natural biomaterials, synthetic polymers and hybrids, ceramics and bioactive glasses (19), the group of natural biomaterials have attracted particular attention due to their low toxicity, low chronic inflammatory response and ability to enhance cell viability, proliferation and differentiation(19). Chitosan (CS) is commonly found in the shells of marine crustaceans, cell walls of fungi and arthropod exoskeleton. It is the deacetylated derivative of chitin, and presents a linear polysaccharide consisting of N-acetyl D-glycosamine and D-glycosamine units (20). CS's biocompatibility, biodegradability, antimicrobial properties, capacity to stimulate macrophages, induce bone formation and interact with negatively charged molecules such as glycosaminoglycans (GAGs) and proteoglycans are the main reasons to account for its widespread use as a biomaterial scaffold (20, 21). The mechanical and biological properties of CS can be further improved by blending it with gelatin (Gel) (22). The latter is another widely studied natural biomaterial deriving from collagen that promotes cell adhesion, proliferation, migration, and differentiation as it retains the Arg-Gly-Asp (RGD) (23). The use of Gel in tissue engineering has also been supported by the fact that it is biodegradable and biocompatible and has low antigenicity, it is commercially available at low cost, does not produce harmful byproducts upon it's enzymatic degradation and contains functional groups for modification (such as crosslinking) and targeting ligands (such as drug delivery vehicles) (23). Although the use of CS:Gel blends results in a better

biological response compared to pure chitosan in bone tissue engineering (24), the instability of the CS:Gel scaffolds in aqueous solutions limit their applications in long-term implantation in vivo. To overcome this limitation, the use of crosslinker molecules has been employed (22). These molecules form intermolecular cross linkages between the polymeric components, thereby improving the mechanical properties of scaffolds and directly affecting their degradation rate (22). Glutaraldehyde is an example of cross-linker that has been widely used in tissue engineering applications (22).

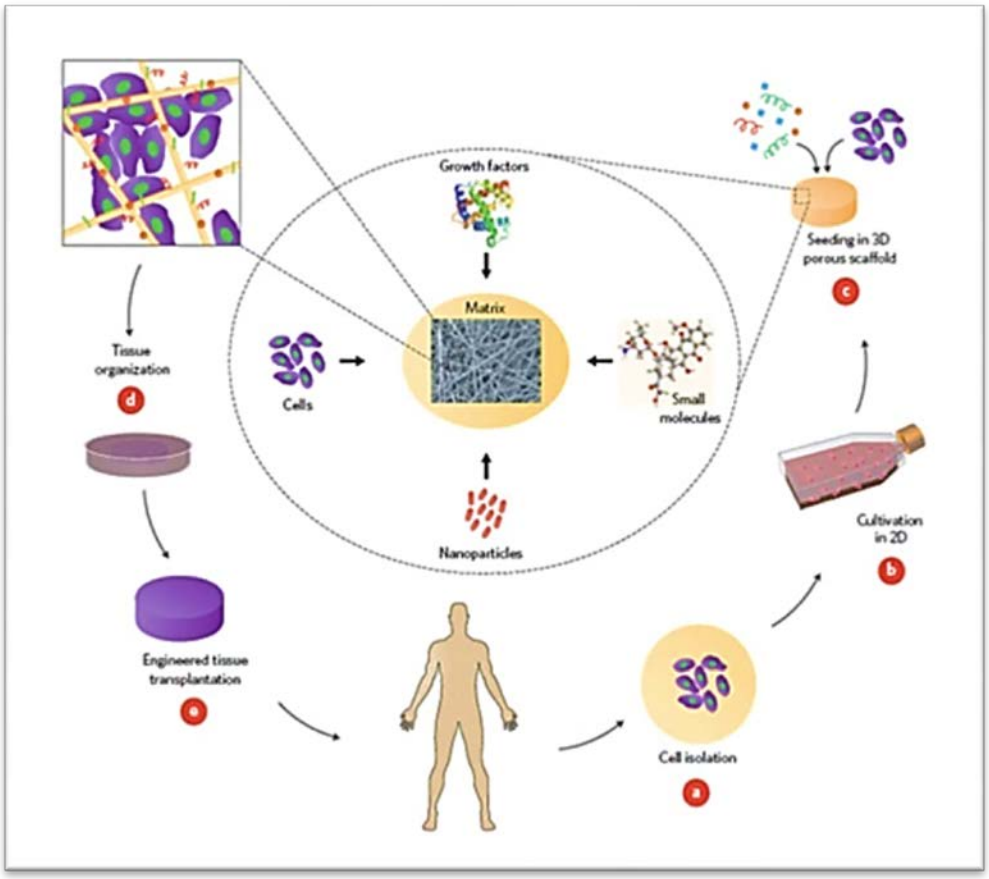

Figure 2: A generic approach of tissue engineering [Nature Nanotechnology, 2010].

Chitosan/gelatin scaffolds for bone regeneration

Our group has recently reported on the fabrication of CS:Gel scaffolds by chemical crosslinking with glutaraldehyde via the use of freeze drying (25) which has been widely used for the fabrication of 3D porous scaffolds over the last 20 years (26). In this technique, samples are cooled at −70°C to −80°C and then they are placed in a

chamber in which the pressure is reduced through a partial vacuum, within which ice from the material is removed by direct sublimation.

CS:Gel scaffolds formed a gel-like structure with interconnected pores, the size of which ranged from 70 to 120 μm (25). The scaffolds supported the strong adhesion and infiltration within the pores of mouse-derived pre-osteoblasts and human BM-MSCs and promoted the survival and proliferation of both cell types. Moreover, they enhanced the levels of collagen secreted into the extracellular matrix by the pre-osteoblasts as compared to the tissue culture polystyrene (TCPS) control surface and furthermore they promoted the osteogenic differentiation of BM-MSCs, as evidenced by the significant increase of the osteogenic gene expression of RUNX2, ALP, and OSC (25). Finally, histological data following implantation of a CS:Gel scaffold into a mouse femur demonstrated that the scaffolds support the formation of ECM, while fibroblasts surrounding the porous scaffold produce collagen with minimal inflammatory reaction (25). Collectively, these results highlight the potential of CS:Gel scaffolds to support new tissue formation and thus provide a promising strategy for bone tissue engineering.

AIM OF THE STUDY

On the basis of data suggesting a promoting role of CS:Gel scaffolds on the formation of ECM by pre-osteoblasts and osteoblasts, the present study aims at extending previous findings, by gaining more insights in the effect of scaffolds on the synthesis and composition of bone ECM. Deciphering the nature of bone ECM and understanding how this may be affected by the substrate is crucial, as bone ECM is not merely a supporting scaffold, but a dynamic and complex structure that regulates osteogenic differentiation, via bidirectional interactions with the cells (27).

Within this context, in the present study we have characterized the composition of ECM produced by BM-MSCs following osteoblastic differentiation in CS:Gel scaffolds. Results were compared with respective cultures in TCPS. To this end, BM samples were obtained from haematologically healthy individuals (n=6) undergoing orthopedic surgery for hip replacement. MSCs were subsequently isolated and cultured as previously described (28), for a total of two passages. Once cultured-expanded cells were identified as bona fide MSCs, based on morphology, immunophenotype and differentiation potential (25, 28-30), they were seeded on CS:Gel scaffolds or on standard TCPS and were induced to undergo osteogenic differentiation as previously described (28, 31). Osteogenesis was assessed by the Alizarin Red and Von Kossa staining methods (28, 31). Furthermore, total RNA from BM- MSCs at the end of differentiation, was isolated and reverse transcribed and subsequently amplified by real-time RT-PCR, for the quantification of genes related to osteogenesis, namely ALP, OSC, DLX5 and RUNX2, using appropriate real-time RT-PCR assays as previously described (25, 30).

To characterize the ECM produced by BM-MSCs differentiated towards osteoblasts, isolated RNA from BM-MSCs seeded on CS:Gel scaffolds or TCPS was used to profile the expression of 29 ECM-related genes via a commercially available PCR array. Additionally, the expression of representative ECM proteins (osteopontin, osteocalcin and collagen 1) by BM-MSCs seeded on scaffold or TCPS and differentiated towards osteoblasts was evaluated by immunofluorescence labeling of these proteins and their visualization under confocal laser fluorescence microscopy.

MATERIALS AND METHODS

1. BM samples

BM samples were isolated from healthy individuals (n=6) undergoing orthopedic surgery for hip replacement. The study had been approved by the Ethics Committee of the University Hospital of Heraklion and informed consent was obtained from all subjects, according to the Helsinki Protocol.

1.a. Protocol of isolation and culture of BM-MSCs

1. Mononuclear cells were isolated from BM samples diluted in complete culture A-MEM with 10% fetal bovine serum (FBS), 100 IU/ml penicillin-streptomycin and 2 mM glutamine (referred as A-MEM medium) (all reagents from Gibco).
2. Diluted sample was layered over Ficoll (Sigma) (ratio 1:1) slowly and angled in order to create two phases.
3. Samples were centrifuged for 30 minutes at 1600 rpm, without brakes, at room temperature.
4. The mesophase/monolayer of monocytes was isolated carefully (**Figure 3**) and the cells were washed with PBS.
5. Centrifugation was followed for 5 minutes at 1500 rpm.
6. Supernatant was removed and the cell pellet was solubilized in PBS.
7. The cells were transferred to flasks (25 cm^2) and plated at a density of $2x10^5$ cells/cm^2 in A-MEM medium and incubated in 37°C/5% CO_2, fully humidified atmosphere.
8. The medium was removed after 24 hours with simultaneous removal of non-adherent cells and refreshment of the medium.
9. On 70-90% confluence, the cells were detached using 0.25% trypsin-1mM EDTA (Gibco) and were sub-cultured thereafter at a density of 2000-3000 cells/cm^2, for 5 passages (P). These adherent cells represent the BM-MSCs.

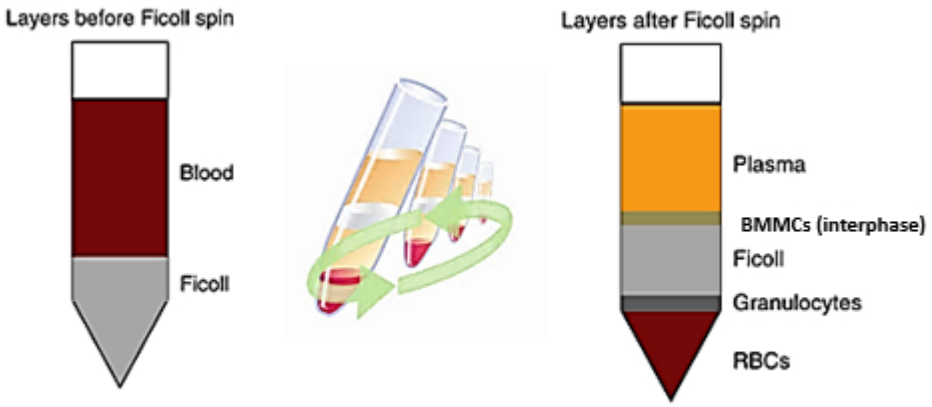

Figure 3. Separation of bone marrow mononuclear cells on Ficoll density gradient.

1. b. Trypsin-EDTA protocol (detaching a confluent BM-MSC surface)

1. The medium was removed from flasks and the flasks were washed with PBS.
2. The PBS was removed, trypsin-EDTA was added and the flasks were incubated for 5 minutes at 37°C.
3. A-MEM medium was added to inactivate Trypsin (2:1, A-MEM:Trypsin-EDTA).
4. Centrifugation followed for 5 minutes, at 1500 rpm, 25°C.
5. The cell pellet was solubilized in the PBS or A-MEM and cells were counted in Neubauer haemocytometer. In specific:
   a) The cells were mixed with Trypan Blue in a proportion 1:1 (10 µl Trypan Blue and 10 µl cell solution).
   b) The cell number was counted according to formula: **n x 2 x 10^4=N cells/ml**
      - n = number of cells in Neubauer
      - N = number of cells per ml
6. The cells were reseeded in 75 cm^2 flask in A-MEM medium and incubated in 37°C/5% CO_2, fully humidified atmosphere.
7. The medium was changed every three days until the next passage (80% confluent surface).

2. Immunophenotypic characterization of BM-MSCs

The immunophenotypic characterization of BM-MSCs was performed by flow cytometry. The panel of antibodies used to characterize MSCs is shown in **Table 1**.

Table 1. Antibodies for flow cytometric characterization of BM-MSCs

Antibodies*	
IgG1 – PE (*Caltac*)	IgG1 – FITC
CD14 – FITC (*Invitrogen*)	CD105 – PE
CD34 – PE	CD29 – FITC
CD45 – FITC	CD73 – PE
CD31 – FITC	CD90 – PE
CD19 – FITC	HLA – DR- PE (*BD Biosciences*)

*The amount of each antibody is 10 µl.
All antibodies are from *Beckman Coulter* unless otherwise stated.
Abbreviations: PE, Phycoerythrin; FITC, Fluoroisothyocyanate.

2.a. Protocol for flow cytometry

1. Test tubes of cytometry were prepared and the BM-MSCs (following a wash to remove excess nutrients) were added at a concentration of $2x10^5$ /tube.
2. The antibodies were added according to manufacturer's instructions.
3. Following vortex, the samples were incubated at 4 °C for 20 minutes, in dark.
4. The samples were washed from the excess amount of unconjugated antibodies using PBS and centrifuged for 5 minutes at 1500 rpm, at 25 °C.
5. The supernatant was removed, the samples were re-diluted in 200-300µl PBS, and were immunophenotypically analyzed (Beckman Coulter Cytomics FC 500).

3. Differentiation of BM-MSCs

3.a. Osteogenesis

BM-MSCs were cultured in 6-well plates until the bottom surface on each well was confluent and then appropriate medium for differentiation into osteocytes was added. Cells were further cultured for 14 days. The osteogenic medium consisted of A-MEM medium as described above (10% FBS, 100 IU/ml penicillin-streptomycin and 2 mM Glutamine) plus 0.1 µM Dexamethasone, 3 mM NaH_2PO_4 (MERCK) and 25 mg/l ascorbic acid (Sigma). For demonstration of osteogenesis we used the Alizarin Red and Von Kossa histochemical stains.

Alizarin Red staining protocol

1. Culture medium was removed and samples were washed twice with PBS.
2. Formaldehyde (4%) was added for 10 minutes.
3. Then formaldehyde was removed and samples were washed with Water for Injection (WFI; highly purified water containing less than 10 CFU/100 ml of Aerobic bacteria) twice.
4. Alizarin Red (2% w/v, pH 4.1-4.3, Sigma) stain was added for 2 – 5 minutes.
5. Alizarin-Red stain was removed and samples were washed twice with WFI.
6. Observation under microscope.

Von Kossa staining protocol

1. Osteogenic medium was removed and samples were washed with PBS twice.
2. Formaldehyde (4%) was added and 10-minute incubation was followed.
3. The formaldehyde was removed and the samples were washed with WFI.
4. Von Kossa (5% w/v aqueous silver nitrate solution) stain was added for 30 minutes at 25 °C in dark.
5. Von Kossa stain was removed and samples were washed twice with WFI.
6. A 15-25-minute exposure at Ultraviolet light was followed.
7. Observation under microscope

3.b. Adipogenesis

BM-MSCs were seeded in 6-well plates until confluence and then suitable medium for adipogenic differentiation was added. Cells were further cultured for 21 days. The adipogenic culture medium consisted of D-MEM (Dulbecco's Modified Eagle's Medium, Gibco) low – glucose with 10% FBS, 100 IU/ml penicillin-streptomycin, 60 mM indomethacin (Sigma), 1 μM dexamethasone and 0.5 mM IBMX. For demonstration of adipogenesis we used the Oil Red O histochemical staining.

Oil Red O staining protocol

1. Oil Red O (1-[2,5-Dimethyl-4-(2,5-dimethylphenylazo)phenylazo]-2-naphthol) (Sigma) stock solution was prepared (0.5% in 99% isopropanol).
2. The adipogenic medium was removed and samples were washed 2x with PBS.
3. 10% Formalin (Sigma-Aldrich) was added and samples were incubated for 15 minutes.

4. Then formalin was removed and samples were washed twice with PBS.
5. At this point the working solution of Oil Red O was prepared as follows: 6 ml of the stock solution were diluted with 4 ml of WFI.
6. After 5 minutes of incubation, working solution was filtered through filter paper and right after through a 0.45 mm filter.
7. Filtered working solution was added in the samples followed by 20-minute incubation.
8. Then samples were washed twice with WFI and were retained at 4 °C for 48 hours.
9. Observation under microscope

4. Assessment of osteogenesis- and adipogenesis-related gene expression by real time reverse transcription-PCR (RT-PCR)

RNA extraction from 10^6 BM-MSCs cells was performed with TRIZOL Reagent (Ambion, Life Technologies), according to manufacturer's instructions. Reverse transcription was performed according to manufacturer's instructions, First – Strand cDNA synthesis SuperScript II RT (Invitrogen).

Protocol for reverse transcription

1. A 20-μL reaction volume was used for 1–500 ng of mRNA. The following components were added to a nuclease-free microcentrifuge tube:
    - 1 μL 50–250 ng random primers
    - x μL 1–500 ng of mRNA
    - 1 μL dNTP Mix (10 mM each) 1 μL
    - Sterile, distilled water to 12 μL
2. Mixture was heated to 65 °C for 5 min and was quickly chilled on ice.
3. Contents were collected and brief centrifugation of the tube was followed. Then the following components were added:
    - 5X First-Strand Buffer 4 μL
    - 0.1 M DTT 2 μL
    - RNaseOUT™ (40 units/μL) (optional)* 1 μL
4. Contents were mixed gently and tubes were incubated at 25 °C for 2 min.

5. 1 µL (200 units) of SuperScript™ II RT was added and mixed by pipetting gently up and down.
6. An incubation at 42 °C for 50 min was followed
7. The reaction was activated by heating at 70 °C for 15 minutes.

Real time RT-PCR protocol

MSCs from passage 2 (P2) were assessed for the expression of genes related to osteogenesis (ALP, OSC, DLX5, RUNX2) and adipogenesis (CCAAT/enhancer-binding protein alpha, CEBPA; Peroxisome Proliferator Activated Receptor gamma, PPARG). RNA was isolated and reverse- transcribed as described above, and 20 ng of cDNA were amplified in each PCR reaction. PCR was performed with KAPA SYBR FAST qPCR Kit Master Mix (Kappa Biosystems, Boston, Massachusetts, USA) and 10 µM of each primer. We used a Rotor-Gene 6000 two-step cycling program consisting of 40 cycles of 95 °C for 3 seconds and 60 °C for 30 seconds. A melting curve (62-95 °C) was generated at the end of each run to verify specificity of the reactions. The forward and reverse primer sequences for PCR amplification are shown in **Table 2**.

Table 2. Primer sequences for real time RT-PCR

	Forward Primer	**Reverse Primer**
ALP*	5’-CCTGCAGCTTCAGAAGCTCAA-3’	5’ACTGTGGAGACACCCATCCC-3’
OSC*	’-GAGGGCAGCGAGGTAGTGAAGA-3’	5’-CGATGTGGTCAGCCAACTCG-3’
DLX5*	5’-CCACCAACCAGCCAGAGAA-3’	5’-CGAGGTACTGAGTCTTCTGAAACC-3’
RUNX2*	5’-GGCCCACAAATCTCAGATCGTT-3’	5’-CACTGGCGCTGCAACAAGAC-3’
CEBPA**	5’-AAGAAGTCGGTGGACAAGAACAC-3’	5’-ACCGCGATGTTGTTGCG-3’
PPARG**	5’-TCAGGGCTGCCAGTTTCG-3’	5’-GCTTTTGGCATACTCTGTGATCTC-3’
GAPDH***	5’-CATGTTCCAATATGATTCCACC-3’	5’-GATGGGATTTCCATTGATGAC-3’

(*) Osteogenesis related genes. (**) Adipogenesis related genes. (***) Normalization control gene.

5. Preparation of the CS/Gel scaffolds

1. CS (Sigma-Aldrich) solution was prepared at 2 % (w/v) by dissolving in 1 % (v/v) acetic acid (Scharlau) in WFI at 37 °C.
2. Gel (Sigma-Aldrich) solution was prepared at 2% (w/v) in WFI at 50°C.

3. The homogenous mixture of CS (40% wt) and Gel (60% wt) was incubated for 2 hours at 50 °C.
4. 0.1% w/v of glutaraldehyde (GA) was added to the CS/Gel mixture.
5. The CS/Gel with GA solution was transferred to the 24-well plates (to form discs for the differentiation assays) and kept overnight at -20 °C.
6. Freeze-drying was followed for 24 hours.

Prior to cell seeding:

1. The scaffolds were neutralized with 0.1 N NaOH (Sigma) solution to remove acetate and a 15-minute incubation, with stirring, was followed.
2. Several washes with WFI were followed till pH reached close to 7.
3. Three washes with PBS were followed, for 30 minutes each, with stirring.
4. Three washes with A-MEM medium were followed, for 30 minutes each, with stirring.
5. Then an overnight incubation of 3D scaffolds with A-MEM medium in 37°C/5% CO_2, fully humidified atmosphere, was followed. After 24 hours the CS:Gel scaffolds were ready for cell seeding.

We examined the support of the above 3D scaffolds in osteogenic differentiation of BM-MSCs as above described (paragraphs 3 and 4).

6. Identification of the extracellular matrix proteins by immunofluoresence

We investigated the endogenous expression of **osteopontin (OPN)** by the BM-MSCs - which were differentiated towards osteoblasts - following culture on the CS:Gel scaffold for 14 days with osteogenic medium, using confocal laser fluorescence microscopy (CLFM). For this purpose, cells were fixed with 4% paraformaldehyde for 15 min followed by permeabilization with 0.1% v/v Triton (Sigma-Aldrich, UK) for 2 h at room temperature, blocking with 10% w/v donkey serum for 4 h at 4 ^{o}C in the dark, overnight incubation at 4 ^{o}C in the dark with mouse anti-osteopontin primary antibody (0.02 mg/ml) (Abcam, Cambridge, USA) in 1% BSA (Sigma-Aldrich (St. Louis, MO, USA), 0.5%Tween20 (Biochemical,BDH Laboratory Supplies,PooleBH15 1TD), 0.01% Sodium azide (Sigma-Aldrich (St. Louis, MO, USA) in PBS. As secondary antibody an Alexa Fluor conjugated anti-mouse antibody (1/200) (Abcam, ab488, Cambridge, USA) was used for 8 h at 4 ^{o}C in the dark. For the stain of the cells'

nucleus we used (4,6-diamidino-2-phenylindole (DAPI) (1:1000) for 12 h at 4 ^{o}C in the dark.

We also investigated by CLFM the endogenous expression of **osteocalcin (OSC)** by the BM-MSCs - which were differentiated towards osteoblasts - following culture on the CS:Gel scaffold for 14 days with osteogenic medium. We followed the same as above described (for osteopontin) procedure using a rabbit anti-osteocalcin primary antibody (5μg/ml) (Abcam, Cambridge, USA) and an Alexa Fluor conjugated anti-rabbit antibody (1/200) (Abcam, ab647, Cambridge, USA) as secondary antibody.

Finally, we investigated by CLFM the endogenous **Collagen 1 A1 (Col1A1)** by the BM-MSCs -which were differentiated towards osteoblasts - following culture on the CS:Gel scaffold for 14 days with osteogenic medium. We followed the same as above procedure using a mouse anti-collagen primary antibody (3 μg/ml) (Abcam, Cambridge, USA) and an Alexa Fluor conjugated anti-mouse antibody (1/200) (Abcam (ab488), Cambridge, USA) secondary antibody.

In all cases, we used the CS:Gel biomaterial with cells without the primary antibody as control.

The expression of osteopontin, osteocalcin and collagen 1 A1 was also evaluated by CLFM in cultures of BM-MSCs which were differentiated towards osteoblasts, following culture in tissue culture polystyrene flasks for 14 days, with osteogenic medium. We used the same procedures, reagents and antibodies. However, following preliminary experiments, we used the secondary antibodies for 3 hours (versus 8 hours in the 3D scaffold) and the DAPI for 5 minutes (versus 12 hours in the 3D scaffold). These cultures were also used as controls for the evaluation of the above protein expression in the CS:Gel scaffolds. **Table 3** shows the antibodies used for immunofluorescence in the 3D scaffold and polystyrene BM-MSC cultures.

Table 3: Reagents used for the immunofluorescence labeling and visualization under a confocal laser scanning microscope.

Antigen	Blocking Serum	Primary Antibody	Secondary Antibody	Company
Osteopontin	Donkey Serum	Mouse Monoclonal (0.02mg/ml)	Donkey Anti-Mouse AF488(1:200)	Abcam
Osteocalcin	Donkey Serum	Rabbit Polyclonal (5µg/ml)	Donkey Anti-Rabbit AF647(1:200)	
Collagen 1 A1	Donkey Serum	Mouse Monoclonal (3µg/ml)	Donkey Anti-Mouse AF488(1:200)	

Abbreviations: AF, Alexa Fluor.

7. Assessment of the ECM and adhesion genes by real time reverse transcription-PCR (RT-PCR)

Total RNA was isolated from osteogenic differentiated BM-MSCs on CS:Gel scaffolds ($n = 6$) and on TCPS control ($n = 6$) cultures at P2 as described above. By using the human Extracellular Matrix & Adhesion Molecules RT^2 Profiler™ PCR Array (SABiosciences, Qiagen) we profiled the expression of 84 genes important for cell-cell and cell-matrix interactions (**Table 4**). The fold change (FC) for each gene between the group of CS:Gel and the group of TCPS differentiated BM-MSCs was calculated with the ΔΔCt method ($FC = 2^{-\Delta\Delta Ct}$). At least a two-fold difference in gene expression between CS:Gel and TCPS BM-MSCs was considered significant.

Procedure

1. **Genomic DNA elimination step**

Total RNA was treated with a DNA elimination step according to manufacturer's instructions. Specifically, an amount of 1 µg total RNA was mixed with 2 µl GE buffer and a variable volume of RNase-free water to a total volume of 10 µl. The DNA elimination mix was incubated for 5 min at 42 ^{o}C, and then was placed immediately on ice for at least 1 min.

2. **Reverse-transcription step**

A 10µl reverse-transcription mix was added to each tube containing genomic DNA elimination mix. After gently mixing by pipetting up and down the final 20 µl

reaction-mix was incubated at 42 ^{o}C for exactly 15 min. Then the reaction was immediately stopped by incubating at 95 ^{o}C for 5 min. 91 µl of RNase-free water were added to each reaction tube. The reactions were placed on ice and preceded with the real-time PCR protocol.

3. Real-Time PCR Using RT^2 qPCR primer assays and RT^2 SYBR Green Mastermixes

The RT^2 SYBR Green Mastermix, RT^2 qPCR Primer Assay, and cDNA synthesis were briefly centrifuged (10-15 sec). The real-time PCR components mix for each reaction was: 12.5 µl RT^2 SYBR Green Mastermix, 1 µl cDNA synthesis reaction, 1 µl RT^2 qPCR Primer Assay (10µM stock). 10.5 µl RNase-free water, in a total volume of 25 µl.

The PCR components mix briefly was centrifuged and placed into the real-time cycler. The program was run according to real-time cycler.

For the Applied Biosystem ViiA7 real-time cycler the cycling conditions were:

a) 1 cycle for 10 min at 95 ^{o}C (activation of HotStart Taq Polymerase by heating step) and

b) 40 cycles for 15 sec at 95 ^{o}C and for 1 min at 60 ^{o}C (fluorescence step/data collection).

A melting curve program run and a first derivative dissociation curve was generated for each well using the real-time cycler software.

Table 4. Gene table of Human Extracellular Matrix & Adhesion Molecules RT^2 Profiler™ PCR Array

Position	Symbol	Description
A01	ADAMTS1	ADAM metallopeptidase with thrombospondin type 1 motif, 1
A02	ADAMTS13	ADAM metallopeptidase with thrombospondin type 1 motif, 13
A03	ADAMTS8	ADAM metallopeptidase with thrombospondin type 1 motif, 8
A04	CD44	CD44 molecule (Indian blood group)
A05	CDH1	Cadherin 1, type 1, E-cadherin (epithelial)
A06	CLEC3B	C-type lectin domain family 3, member B
A07	CNTN1	Contactin 1
A08	COL11A1	Collagen, type XI, alpha 1
A09	COL12A1	Collagen, type XII, alpha 1
A10	COL14A1	Collagen, type XIV, alpha 1
A11	COL15A1	Collagen, type XV, alpha 1
A12	COL16A1	Collagen, type XVI, alpha 1
B01	COL1A1	Collagen, type I, alpha 1
B02	COL4A2	Collagen, type IV, alpha 2
B03	COL5A1	Collagen, type V, alpha 1

B04	COL6A1	Collagen, type VI, alpha 1
B05	COL6A2	Collagen, type VI, alpha 2
B06	COL7A1	Collagen, type VII, alpha 1
B07	COL8A1	Collagen, type VIII, alpha 1
B08	CTGF	Connective tissue growth factor
B09	CTNNA1	Catenin (cadherin-associated protein), alpha 1, 102kDa
B10	CTNNB1	Catenin (cadherin-associated protein), beta 1, 88kDa
B11	CTNND1	Catenin (cadherin-associated protein), delta 1
B12	CTNND2	Catenin (cadherin-associated protein), delta 2 (neural plakophilin-related arm-repeat protein)
C01	ECM1	Extracellular matrix protein 1
C02	FN1	Fibronectin 1
C03	HAS1	Hyaluronan synthase 1
C04	ICAM1	Intercellular adhesion molecule 1
C05	ITGA1	Integrin, alpha 1
C06	ITGA2	Integrin, alpha 2 (CD49B, alpha 2 subunit of VLA-2 receptor)
C07	ITGA3	Integrin, alpha 3 (antigen CD49C, alpha 3 subunit of VLA-3 receptor)
C08	ITGA4	Integrin, alpha 4 (antigen CD49D, alpha 4 subunit of VLA-4 receptor)
C09	ITGA5	Integrin, alpha 5 (fibronectin receptor, alpha polypeptide)
C10	ITGA6	Integrin, alpha 6
C11	ITGA7	Integrin, alpha 7
C12	ITGA8	Integrin, alpha 8
D01	ITGAL	Integrin, alpha L (antigen CD11A (p180), lymphocyte function-associated antigen 1; alpha polypeptide)
D02	ITGAM	Integrin, alpha M (complement component 3 receptor 3 subunit)
D03	ITGAV	Integrin, alpha V (vitronectin receptor, alpha polypeptide, antigen CD51)
D04	ITGB1	Integrin, beta 1 (fibronectin receptor, beta polypeptide, antigen CD29 includes MDF2, MSK12)
D05	ITGB2	Integrin, beta 2 (complement component 3 receptor 3 and 4 subunit)
D06	ITGB3	Integrin, beta 3 (platelet glycoprotein IIIa, antigen CD61)
D07	ITGB4	Integrin, beta 4
D08	ITGB5	Integrin, beta 5
D09	KAL1	Kallmann syndrome 1 sequence
D10	LAMA1	Laminin, alpha 1
D11	LAMA2	Laminin, alpha 2
D12	LAMA3	Laminin, alpha 3
E01	LAMB1	Laminin, beta 1
E02	LAMB3	Laminin, beta 3
E03	LAMC1	Laminin, gamma 1 (formerly LAMB2)
E04	MMP1	Matrix metallopeptidase 1 (interstitial collagenase)
E05	MMP10	Matrix metallopeptidase 10 (stromelysin 2)
E06	MMP11	Matrix metallopeptidase 11 (stromelysin 3)
E07	MMP12	Matrix metallopeptidase 12 (macrophage elastase)
E08	MMP13	Matrix metallopeptidase 13 (collagenase 3)
E09	MMP14	Matrix metallopeptidase 14 (membrane-inserted)
E10	MMP15	Matrix metallopeptidase 15 (membrane-inserted)
E11	MMP16	Matrix metallopeptidase 16 (membrane-inserted)
E12	MMP2	Matrix metallopeptidase 2 (gelatinase A, 72kDa gelatinase, 72kDa type IV collagenase)
F01	MMP3	Matrix metallopeptidase 3 (stromelysin 1, progelatinase)
F02	MMP7	Matrix metallopeptidase 7 (matrilysin, uterine)
F03	MMP8	Matrix metallopeptidase 8 (neutrophil collagenase)
F04	MMP9	Matrix metallopeptidase 9 (gelatinase B, 92kDa gelatinase,

		92kDa type IV collagenase)
F05	NCAM1	Neural cell adhesion molecule 1
F06	PECAM1	Platelet/endothelial cell adhesion molecule
F07	SELE	Selectin E
F08	SELL	Selectin L
F09	SELP	Selectin P (granule membrane protein 140kDa, antigen CD62)
F10	SGCE	Sarcoglycan, epsilon
F11	SPARC	Secreted protein, acidic, cysteine-rich (osteonectin)
F12	SPG7	Spastic paraplegia 7 (pure and complicated autosomal recessive)
G01	SPP1	Secreted phosphoprotein 1
G02	TGFBI	Transforming growth factor, beta-induced, 68kDa
G03	THBS1	Thrombospondin 1
G04	THBS2	Thrombospondin 2
G05	THBS3	Thrombospondin 3
G06	TIMP1	TIMP metallopeptidase inhibitor 1
G07	TIMP2	TIMP metallopeptidase inhibitor 2
G08	TIMP3	TIMP metallopeptidase inhibitor 3
G09	TNC	Tenascin C
G10	VCAM1	Vascular cell adhesion molecule 1
G11	VCAN	Versican
G12	VTN	Vitronectin

8. Statistical Analysis

Statistical analysis was performed using the GraphPad Prism version 6 software. We used the Wilcoxon test for paired samples to check the differences in the expression of adipogenesis and osteogenesis genes between different time-points during differentiation of BM-MSCs. We used Mann Whitney test to evaluate the differences in the mean relative expression of osteogenesis related genes between experimental time-points (day 7 or day 14 versus day 0) in the CS:Gel scaffold or between the CS:Gel scaffold and the TCPS control. A p value < 0.05 was considered statistically significant.

APPENDIX OF THE TECHNIQUES

Flow cytometry

Flow cytometry measures optical and fluorescence characteristics of single cells. Inside a flow cytometer, cells in suspension are drawn into a stream created by a surrounding sheath of isotonic fluid that creates laminar flow, allowing the cells to pass individually through an interrogation point. At the interrogation point, a beam of monochromatic light, usually from a laser, intersects the cells. Emitted light is given off in all directions and is collected via optics that direct the light to a series of filters and dichroic mirrors that isolate particular wavelength bands. The light signals are detected by photomultiplier tubes and digitized for computer analysis. The resulting information usually is displayed in histogram or two-dimensional dot-plot formats (**Figure 4**).

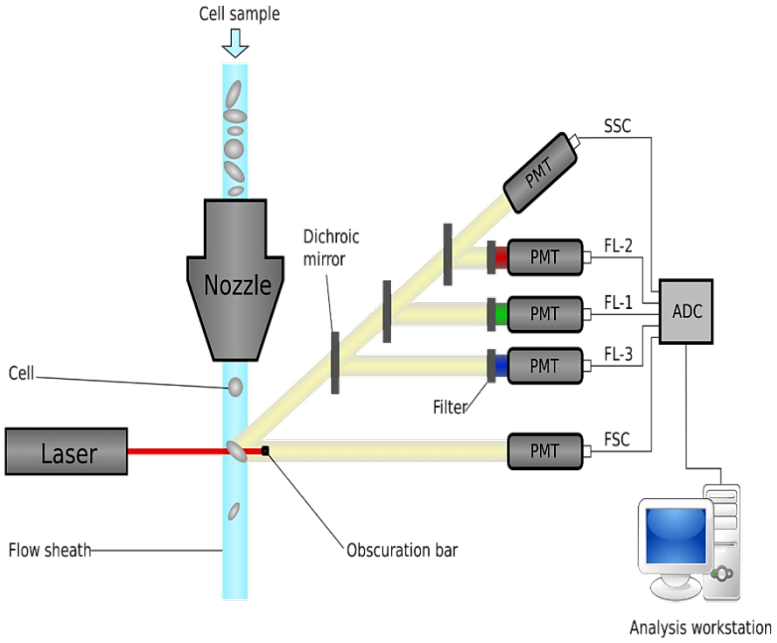

Figure 4. Flow-cytometer [https://en.wikipedia.org/wiki/Flow_cytometry_bioinformatics]

Freeze Dryer

Freeze drying is the removal of ice or other frozen solvents from a material through the process of sublimation and the removal of bound water molecules through the process of desorption. Lyophilization and freeze drying are terms that are used

interchangeably depending on the industry and location where the drying is taking place. Controlled freeze drying keeps the product temperature low enough during the process to avoid changes in the dried product appearance and characteristics. It is an excellent method for preserving a wide variety of heat-sensitive materials such as proteins, microbes, pharmaceuticals, tissues and plasma (**Figure 5**).

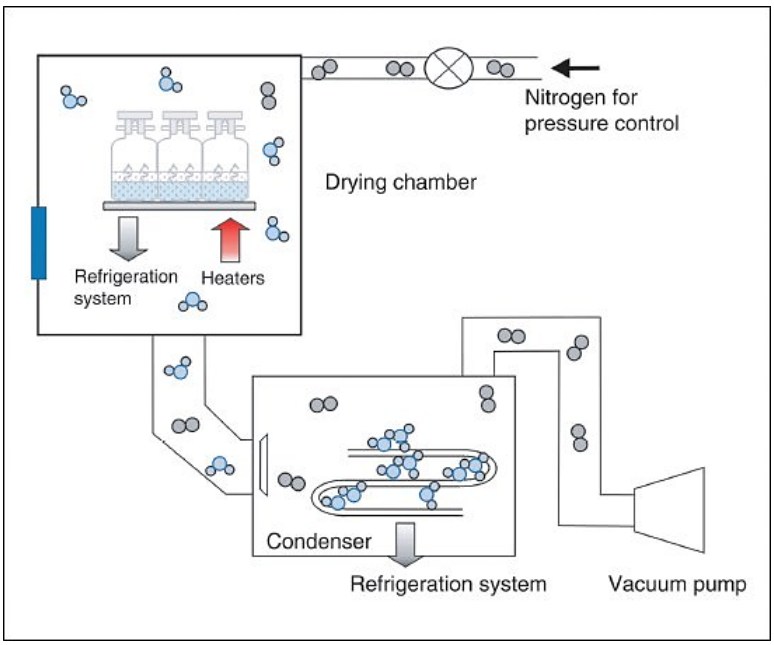

Figure 5. Example of a lyophilization unit operation.
(http://www.biopharminternational.com)

Sublimation

Sublimation is when a solid (ice) changes directly to a vapor without first going through a liquid (water) phase. Thoroughly understanding the concept of sublimation is a key building block to gaining knowledge of freeze drying. Sublimation is a phase change and heat energy must be added to the frozen product for it to occur. Sublimation in the freeze-drying process can be described simply as:

Freeze - The product is completely frozen, usually in a vial, flask or tray.

Vacuum - The product is then placed under a deep vacuum, well below the triple point of water.

Dry – Heat energy is then added to the product causing the ice to sublime.

Scanning Electron Microscopy (SEM)

The SEM gives information about the topology of the sample. A beam of electrons is produced at the top of the microscope by an electron gun. The electron beam follows a vertical path through the microscope, which is held within a vacuum. The beam travels through electromagnetic fields and lenses, which focus the beam down toward the sample. Once the beam hits the sample, electrons and X-rays are ejected from the sample. Detectors collect these X-rays, backscattered electrons, and secondary electrons and convert them into a signal that is sent to a screen similar to a television screen (**Figure 6**).

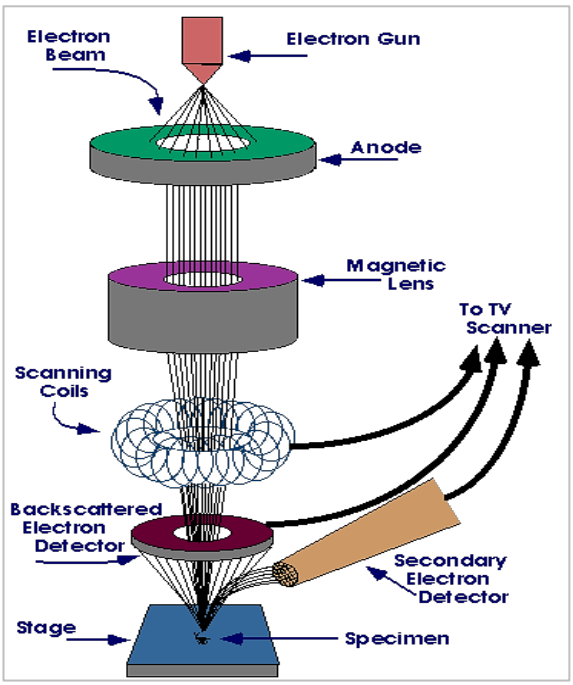

Figure 6. Main parts of a Scanning Electron Microscope
[http://www.slideshare.net/DiegoRamos5/microscopy-15336091]

Confocal Laser Scanning Microscopy (CLSM)

CLSM combines high-resolution optical imaging with depth selectivity which allows us to do optical sectioning. This means that we can view visual sections of tiny structures that would be difficult to physically section and construct 3D structures from the obtained images (**Figure 7**).

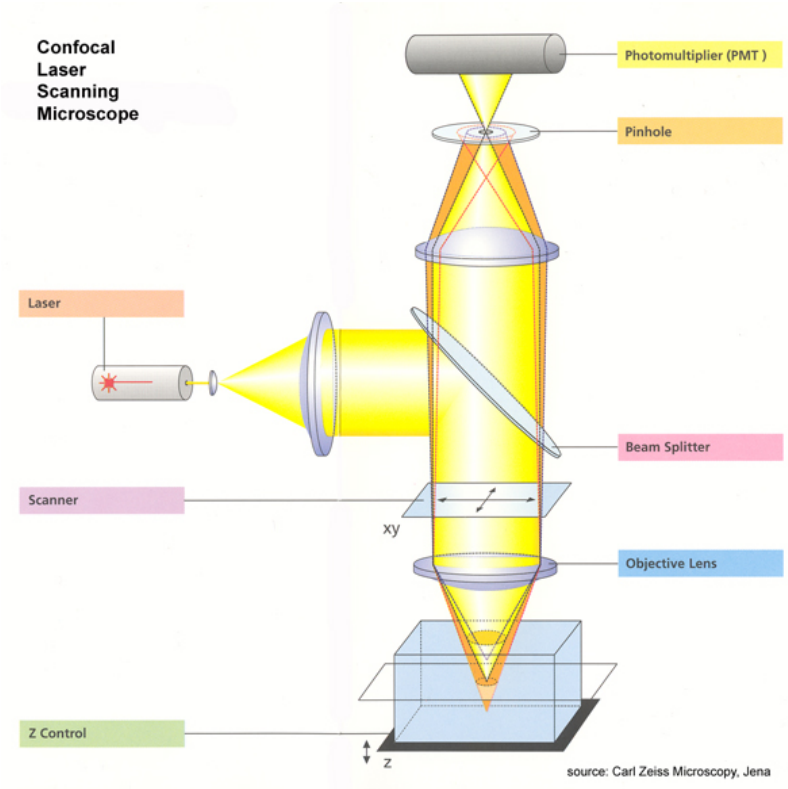

Figure 7. Main parts of a Confocal Laser Scanning Microscope [https://bitesizebio.com/19958/what-is-confocal-laser-scanning-microscopy/]

RESULTS

1. Morphology, immunophenotype and differentiation potential of BM-MSCs

BM-MSCs from 6 healthy individuals were isolated and cultured successfully *ex-vivo*. According to the criteria for the definition of MSCs, our BM-MSCs were (a) adherent to the plastic, (b) displayed the characteristic spindle-like morphology **(Figure 8)** and (c) expressed the characteristic phenotype. In specific, at passage (P) 2, our cells were immunophenotypically analyzed for the expression of cell surface markers using flow cytometry and the results showed that the cultures contained a homogeneous cell population positive for the mesenchymal markers CD105, CD90 and CD73 and negative for the haemopoietic markers CD14, CD34, CD45 **(Fig**

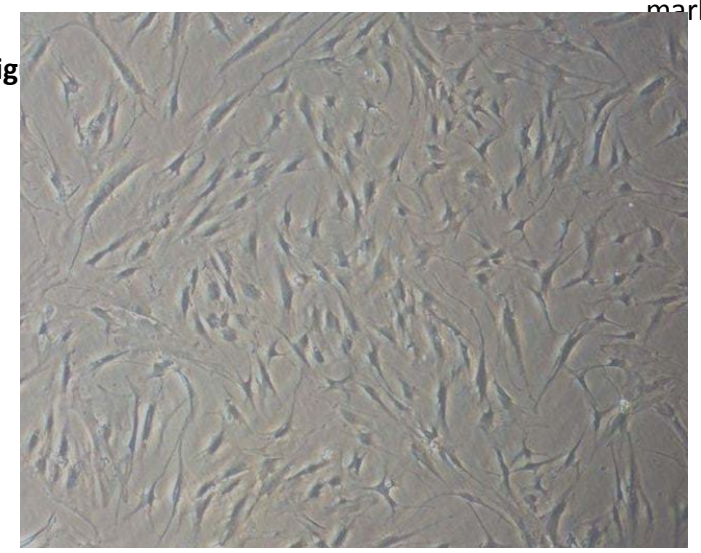

Figure 8: Cultured BM-MSCs at passage 2 (P2).

Furthermore, the cells had the capacity to differentiate into osteocytes and adipocytes as was observed with the appropriate staining, namely Alizarin Red and Von Kossa for osteocytes **(Figure 10)** and Oil Red for adipocytes **(Figure 11)**. Alizarin Red stains the mineralized matrix of the osteocytes, Von Kossa the hydroxyapatite of the osteocytes and Oil Red the lipid droplets of the adipocytes.

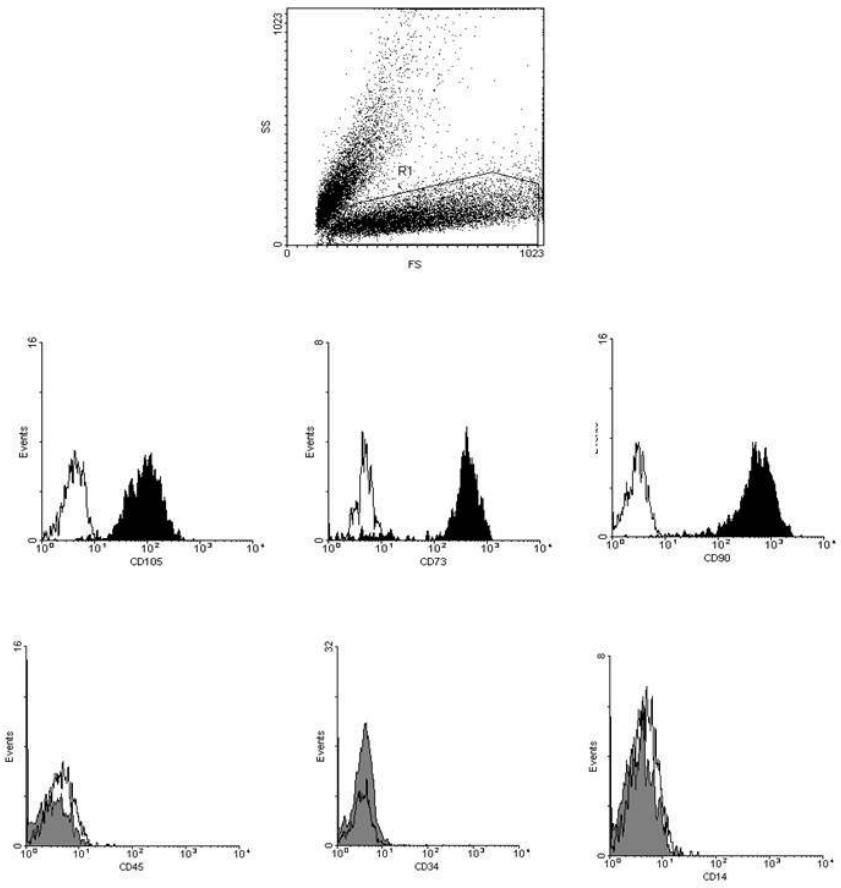

Figure 9: Immunophenotypic analysis of cultured BM-MSCs at P2. The upper diagram shows the Forward Scatter (FS) and Side Scatter (SS) properties of the cells and the lower diagrams the positive (CD105, CD73, CD90) and negative (CD45, CD34, CD14) markers.

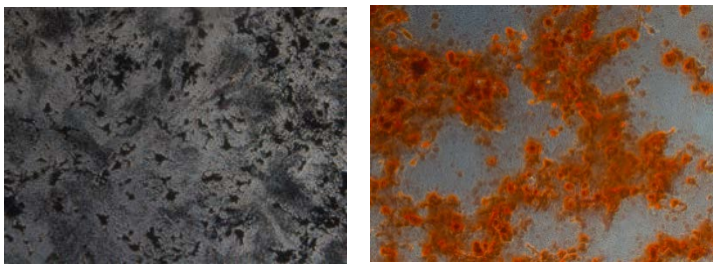

Figure 10: Von Kossa and Alizarin Red of BM-MSCs cultured for 14 days in osteogenic medium (magnification 10x).

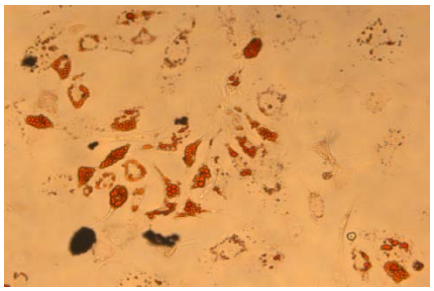

Figure 11: Oil Red O of BM-MSCs cultured for 21 days in adipogenic medium (magnification 10x).

The capacity of culture-expanded BM-MSCs to differentiate into adipocytes and osteocytes was also evaluated by the expression of adipogenesis- and osteogenesis-related genes. For adipogenesis, two genes were studied, PPARG and CEBPA, the key transcription factors of adipogenesis. Real time RT-PCR assays were performed to evaluate the expression of the adipogenic markers at day 0 (induction of differentiation) which was the control and day 14. Each RT-PCR assay was performed in triplicate. As shown in **Figure 12** both PPARG and CEBPA expression progressively increased during the 14-day culture in adipocytic medium indicating that all the cultured MSCs differentiated in adipocytes.

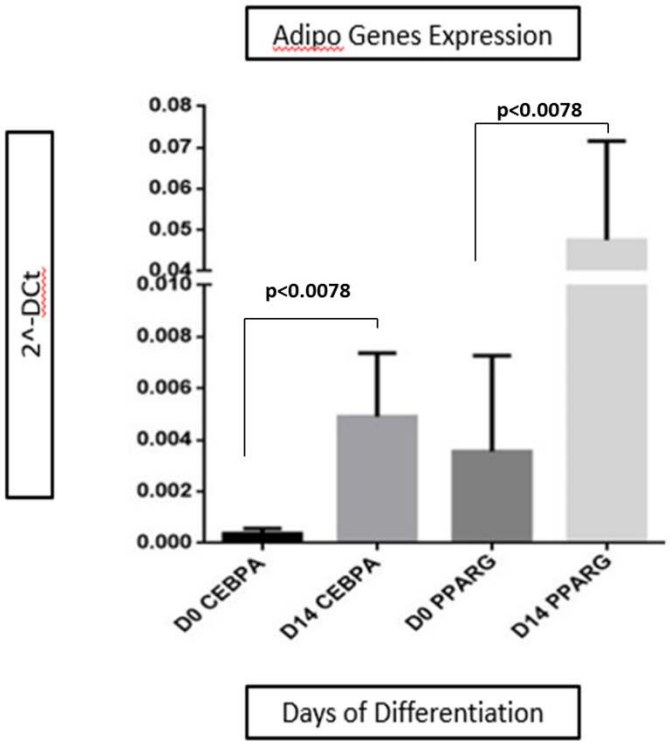

Figure 12: Real time RT-PCR analysis of adipogenesis-related genes (2-ΔCt method using GAPDH as control gene). The bars represent the mean (+ 1 standard deviation, SD) expression of CEBPA and PPARG mRNA levels of culture-expanded BM MSCs from 6 healthy individuals prior (day 0) and during adipogenic differentiation (day 14). Differences between day 0 and day 14 were statistically significant for both CEBPA and PPARG (Wilcoxon paired test).

For osteogenesis four genes were studied, RUNX2, ALP, DLX5 and OSC. RUNX2 is the master transcription factor regulating early osteogenesis (32). DLX5 induces osteoblast maturation by triggering the expression of RUNX2 and ALP and thus

supports osteogenesis. ALP is a key enzyme that provides high concentrations of phosphate at the site of mineral deposition in active osteoblasts and is considered a marker of early osteogenesis (32). Finally, OSC is secreted solely by osteoblasts and is implicated in bone mineralization and calcium ion homeostasis (32). Real time RT-PCR assays were performed to evaluate the expression of the osteogenic markers at day 0 (induction of differentiation) which was the control and 14. Each RT-PCR assay was performed in triplicate. As shown in **Figure 13** all the above genes' expression was increased during the 14-day culture in osteocytic medium demonstrating that cultured MSCs differentiated in osteocytes.

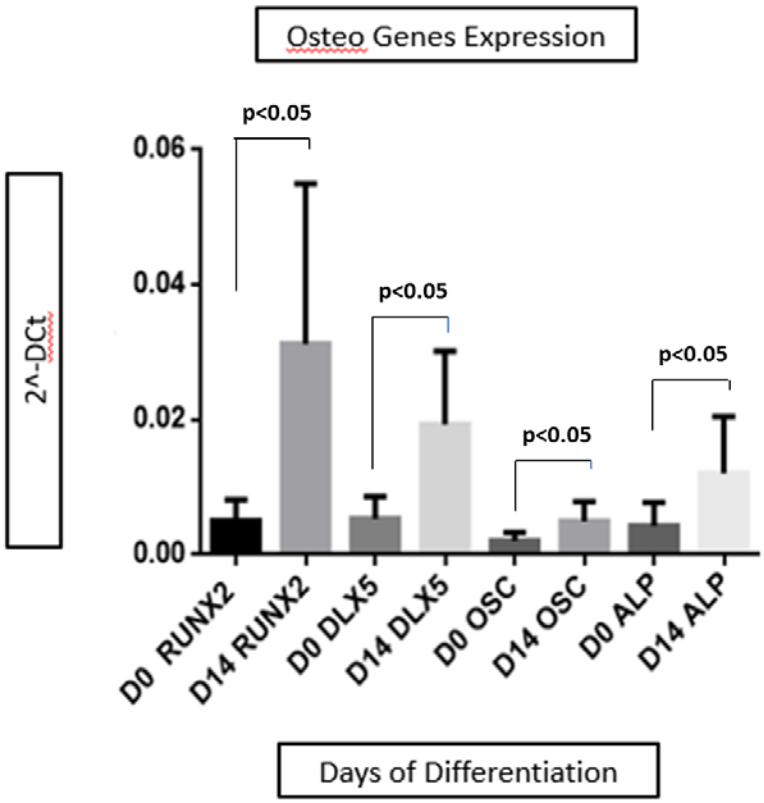

Figure 13: Real time RT-PCR analysis of osteogenesis-related genes (2-ΔCt method using GAPDH as control gene). The **bars represent the mean** (+ 1 standard deviation, SD) expression of RUNX2, DLX5, OSC and ALP mRNA of culture-expanded BM MSCs from 6 healthy individuals prior (day 0) and during osteogenic differentiation (day 14). Differences between day 0 and day 14 were statistically significant for all genes (Wilcoxon paired test).

2. Chitosan-Gelatin (CS:Gel) 3D scaffolds and BM-MSCs

2a. Morphological characteristics of the scaffold and effect on BM-MSC adhesion

We investigated the porous size and the morphology of our CS:Gel scaffold (40%C-

60%G) after 24 hours of lyophilization. SEM analysis showed that the structure of scaffold maintains uniform pore sizes throughout the surface and displays homogeneous morphology without any salt accumulation (**Figure 14).**

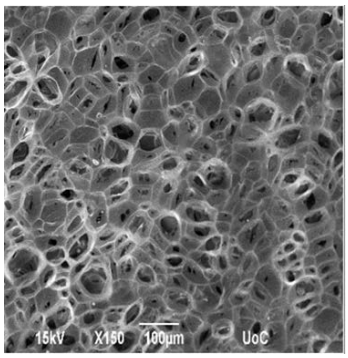

Figure 14: Scanning Electron Microscopy (SEM) image showing a 3D porous chitosan-gelatin scaffold with a 40:60% ratio after lyophilization (150-fold magnification).

Moreover, to examine the BM-MSC viability and adhesion, 10^5 undifferentiated P2 BM-MSCs expanded in A-MEM proliferation medium were seeded in the CS:Gel scaffolds and placed at 37 ^{o}C in a cell culture incubator. SEM images show the adhesion of the cells in the scaffold (**Figure 15).** After three days of culture, the surface of the scaffold was fully covered by BM-MSCs. Furthermore, adhered cells formed cytoplasmic connections, thereby enabling their organization into tissue.

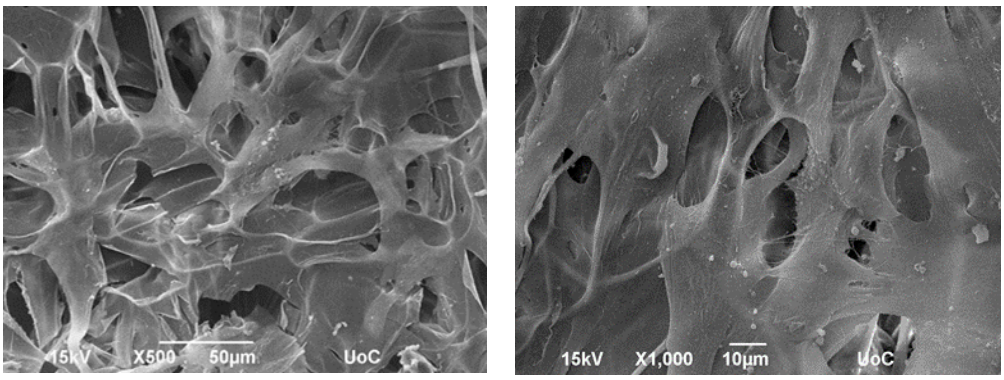

Figure 15: Scanning Electron Microscopy images showing undifferentiated BM-MSCs cultured on chitosan-gelatin scaffolds (40:60% ratio) after two-day incubation with A-MEM medium following air drying. (Left) 500-fold magnification and (right) 1000-fold magnification.

2b. Osteogenic differentiation potential of BM-MSCs on the 3D CS:Gel scaffolds

To investigate the potential of the BM-MSCs to differentiate into osteocytes on the CS:Gel scaffolds, cells from six (6) healthy donors were seeded on the scaffold for 3

days using A-MEM. Then the medium was changed to osteogenic medium for 14 days.

Furthermore, real time RT-PCR assays were performed to evaluate the gene expression of the same osteogenic markers as in the polystyrene namely RUNX2, ALP, DLX5 and OSC at days 7 and 14 and day 0 as a control. Day 0 is the time point before the start of the differentiation.

As shown in **Figure 16** the mean relative expression of RUNX2, ALP, OSC and DLX5 increased significantly during the 14 day culture of BM-MSCs on the CS:Gel scaffold in the presence of osteogenic medium compared to day 0. In all cases the differences between the day 7 and day 0 as well as between day 14 and day 0 were statistically significant. These data suggest that the CS:Gel scaffold strongly supports the differentiation of BM-MSCs towards osteocytes.

The comparison in the mean relative RUNX2, ALP, OSC and DLX5 expression of BM-MSCs between CS:Gel scaffold and polystyrene during the 14-day culture in the osteogenic medium showed statistically significant increased expression of ALP and OSC in the scaffold at both day 7 and day 14. RUNX2 expression in the CS:Gel scaffold at day 7 was also increased compared to polystyrene but not at a statistically significant level whereas no differences were obtained in DLX5 expression. The significant increased ALP and OSC expression indicates that the CS:Gel scaffold with GA as crosslinker favors the osteogenic differentiation of BM-MSCs as compared to the polystyrene control.

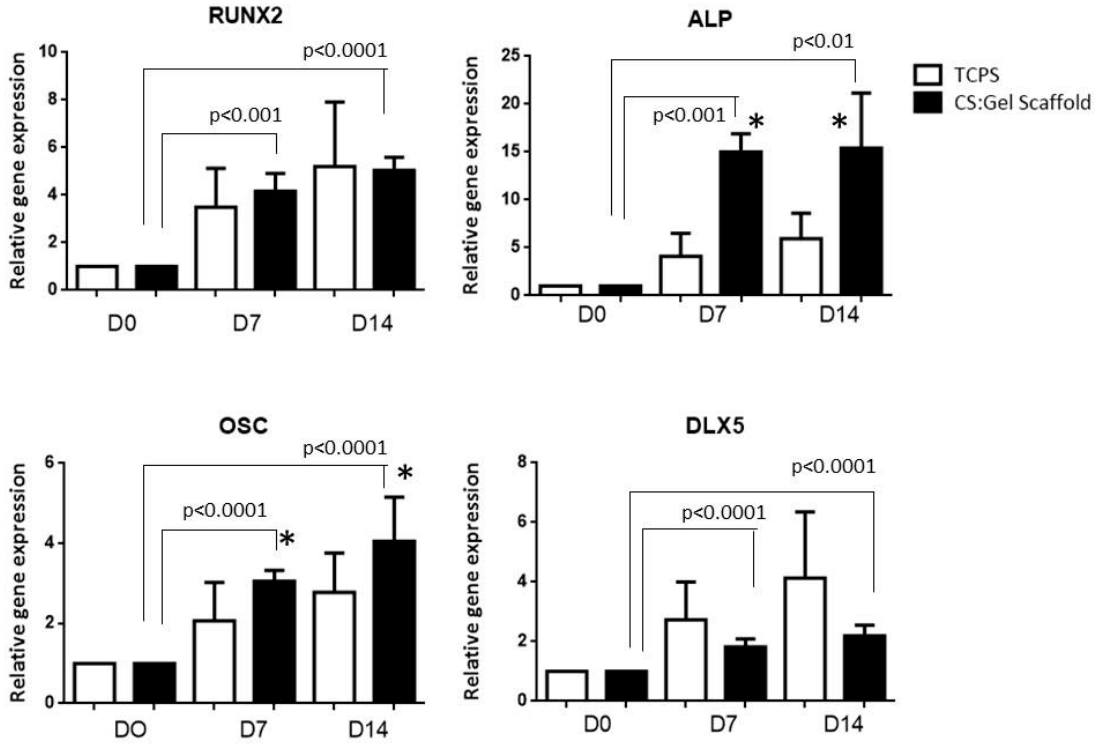

Figure 16: **Relative osteogenic gene expression in BM-MSCs cultured in osteogenic medium for 7 and 14 days on chitosan-gelatin (CS:Gel) scaffold versus tissue culture polystyrene (TCPS) control.** The bars represent the mean (+ 1 standard deviation, SD) RUNX2, ALP, OSC and DLX5 expression using quantitative real-time PCR at days 0 and days 7 and 14 of differentiation (n=6). Relative gene expression levels were analyzed using the method $2^{-\Delta\Delta Ct}$ by normalizing with the housekeeping gene GAPDH as an endogenous control. The ΔCt value for a target gene in a specific sample was obtained by subtracting the GAPDH Ct value from the gene Ct value. The ΔΔCt was determined by subtracting the ΔCt of the specific sample from the ΔCt of the control sample, which is BM-MSCs just before they underwent osteogenic differentiation (day 0). The p values show the differences in the relative gene expression at day 7 or day 14 compared to day 0 in BM-MSCs cultured in the CS:Gel scaffold (Mann Whitney test). Asterisks show the statistically significant differences in ALP and OSC expression of BM-MSCs cultured in the scaffold vs the TCPS at the respective days of culture (Mann Whitney test).

3. Expression of ECM proteins using confocal laser fluorescence microscope (CLFM)

The expression of proteins which have relation with ECM was examined using CLFM in both the TCPS and CS:Gel biomaterial (**Figure 17** and **Figure 18**). In both experimental groups the cell nucleus was stained by Dapi (blue), osteocalcin by Alexa Fluor 647 (red), collagen type I A1 by Alexa Fluor 488 (green) and osteopontin also by Alexa Fluor 488 (green). As shown in **Figure 17,** collagen type I A1 and osteopontin were strongly expressed in the TCPS whereas osteocalcin was expressed at a lower

level. Similarly, in the CS:Gel biomaterial (**Figure 18**) collagen type I A1 and osteopontin were strongly expressed whereas osteocalcin was expressed at a lower level. Although a more intense expression of collagen type I A1 and osteopontin was seen in TCPS compared to CS:Gel scaffold, the staining methods are different and any comparison might be inaccurate. Anyhow, the above findings of the collagen type I A1 and osteopontin protein expression provides additional evidence that our CS-Gel scaffold with glutalardeyde as crosslinker supports osteogenesis. The lower expression of osteocalcin in both biomaterial and polystyrene might be due to the fact that this protein is a late marker of osteogenic differentiation expressed at a higher level after the second week of osteogenic induction. Nevertheless, for the experiments presented herein, cells were differentiated for two weeks as commonly performed in relevant tissue engineering literature.

4. Differential expression of ECM associated genes between BM-MSCs induced to undergo osteogenic differentiation on scaffolds or TCPS

We have evaluated the expression of 84 genes associated with ECM and adhesion using a PCR array. In the present study we focused on 29 genes associated with bone ECM according to the literature (Table 5) and further analysis was restricted to this subset (Table 9). By considering as significant an at least 2- or ½-fold change (FC) in gene expression between BM-MSCs induced to undergo osteogenic differentiation on CS:Gel scaffolds (scaffold group) and those cultured on TCPS (control group)(33, 34) we observed that 28/29 genes were differentially expressed between the two experimental groups. Fold-change values greater than 2 are indicated in red; fold-change values less than 0.5 are indicated in blue (Table 9). More precisely, 9 genes were upregulated and 19 genes downregulated in BM-MSCs undergoing osteogenic differentiation on scaffolds (Figure 19). However, when comparisons are made one should bear in mind that the average threshold cycle of nearly all evaluated genes in BM-MSCs cultured on scaffolds (scaffold group) was relatively high (>30), meaning that their relative expression level is low.

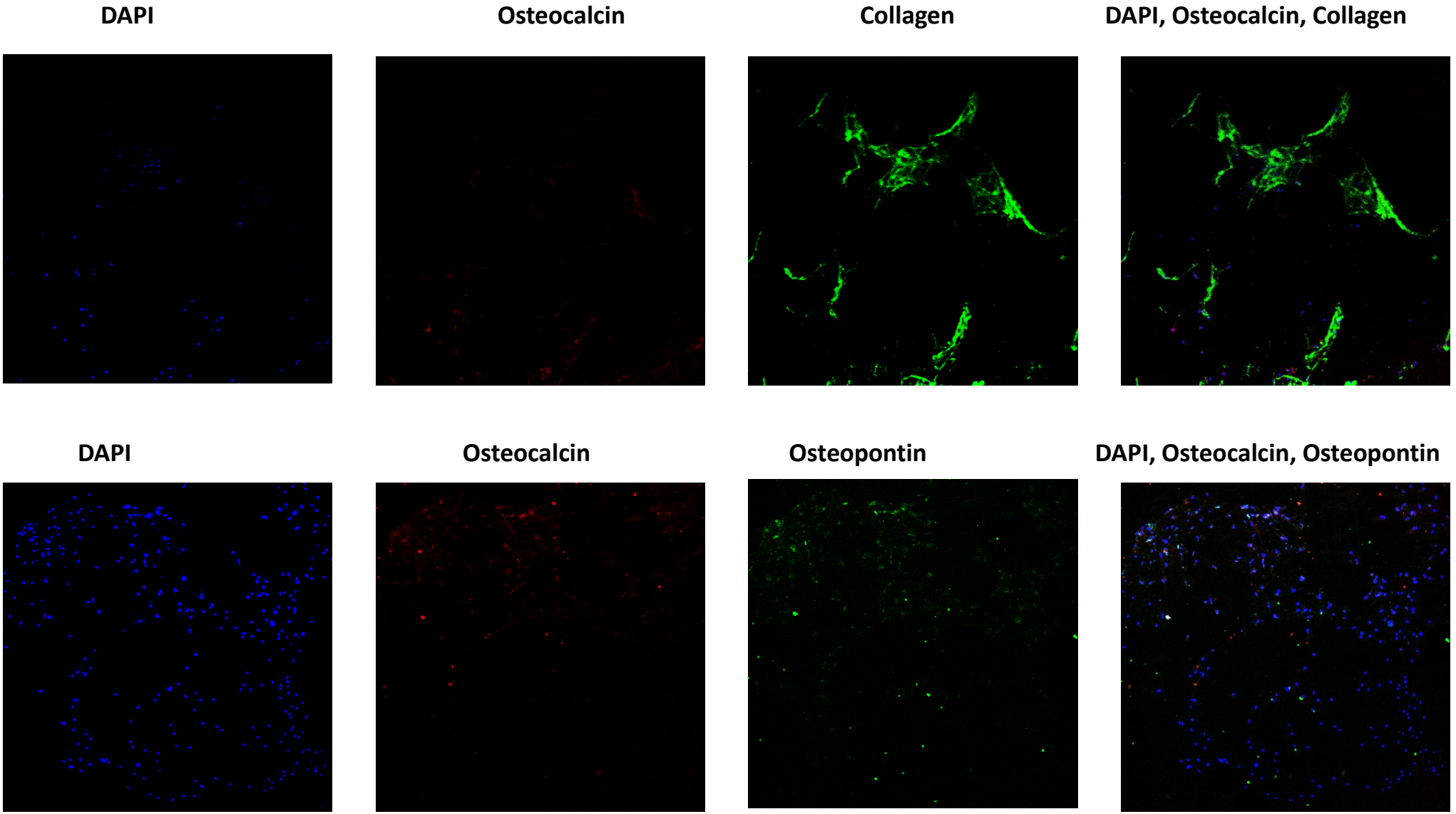

Figure 17: ECM proteins using confocal laser fluorescence microscopy in cultures of BM-MSCs in polystyrene. The upper Figures show staining of cells' nucleus with dapi, expression of osteocalcin, collagen I A1 and an overlay of the three stains, respectively. The lower Figures show staining of cells' nucleus with dapi, expression of osteocalcin, osteopontin, and an overlay of the three stains, respectively. Magnification 10x in all cases.

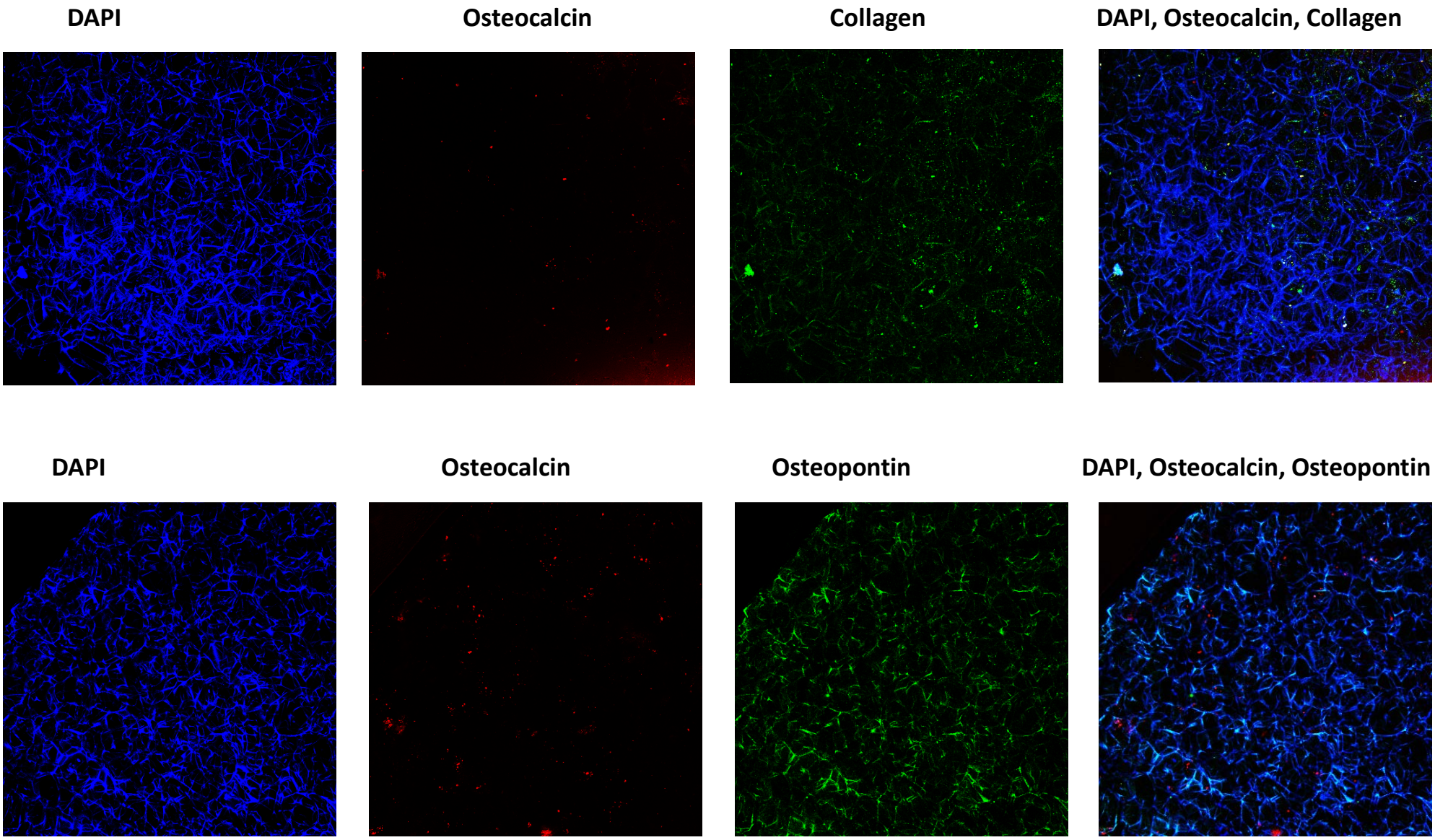

Figure 18: ECM proteins using confocal laser fluorescence microscopy in cultures of BM-MSCs in CS:Gel scaffolds. The upper Figures show staining of cells' nucleus with dapi, expression of osteocalcin, collagen I A1 and an overlay of the three stains, respectively. The lower Figures show staining of cells' nucleus with dapi, expression of osteocalcin, osteopontin, and an overlay of the three stains, respectively. Magnification of 10x in all cases.

Table 9. Fold change of the expression of genes related to bone ECM in BM-MSCs undergoing osteogenic differentiation on CS:Gel scaffolds as compared to tissue culture polystyrene control.

Symbol	Description	BM-MSCs	
		Fold Change	95% CI
ADAMTS1	ADAM metallopeptidase with thrombospondin type 1 motif, 1	0.0085	(0.00001, 0.03)
CLEC3B	C-type lectin domain family 3, member B	0.0135	(0.00001, 0.03)
COL1A1	Collagen, type I, alpha 1	0.0042	(0.00, 0.01)
COL5A1	Collagen, type V, alpha 1	0.0833	(0.00001, 0.17)
CTGF	Connective tissue growth factor	0.0005	(0.00001, 0.00)
ECM1	Extracellular matrix protein 1	0.0127	(0.01, 0.02)
FN1	Fibronectin 1	0.0004	(0.00001, 0.00)
MMP1	Matrix metallopeptidase 1 (interstitial collagenase)	5.4095	(0.00001, 11.23)
MMP10	Matrix metallopeptidase 10 (stromelysin 2)	2.0403	(0.00001, 4.55)
MMP11	Matrix metallopeptidase 11 (stromelysin 3)	6.1322	(0.10, 12.17)
MMP12	Matrix metallopeptidase 12 (macrophage elastase)	6.0915	(0.00001, 30.92)
MMP13	Matrix metallopeptidase 13 (collagenase 3)	2.193	(0.10, 4.28)
MMP14	Matrix metallopeptidase 14 (membrane-inserted)	0.085	(0.05, 0.12)
MMP16	Matrix metallopeptidase 16 (membrane-inserted)	3.5588	(0.25, 6.86)
MMP2	Matrix metallopeptidase 2 (gelatinase A, 72kDa gelatinase, 72kDa type IV collagenase)	0.0224	(0.01, 0.03)
MMP3	Matrix metallopeptidase 3 (stromelysin 1, progelatinase)	2.9184	(0.00001, 7.44)
MMP9	Matrix metallopeptidase 9 (gelatinase B, 92kDa gelatinase, 92kDa type IV collagenase)	14.7874	(0.00001, 32.65)
SPARC	Secreted protein, acidic, cysteine-rich (osteonectin)	0.0019	(0.00001, 0.01)
SPP1	Secreted phosphoprotein 1 (osteopontin)	0.1116	(0.02, 0.21)
TGFBI	Transforming growth factor, beta-induced, 68kDa	0.001	(0.00001, 0.00)
THBS1	Thrombospondin 1	0.0009	(0.00, 0.00)
THBS2	Thrombospondin 2	0.0468	(0.03, 0.06)
TIMP1	TIMP metallopeptidase inhibitor 1	0.001	(0.00001, 0.00)
TIMP2	TIMP metallopeptidase inhibitor 2	0.006	(0.00, 0.01)
TIMP3	TIMP metallopeptidase inhibitor 3	0.0035	(0.00001, 0.01)
TNC	Tenascin C	0.0055	(0.00, 0.01)
VCAN	Versican	0.0004	(0.00, 0.00)
VTN	Vitronectin	3.4115	(0.00001, 12.34)

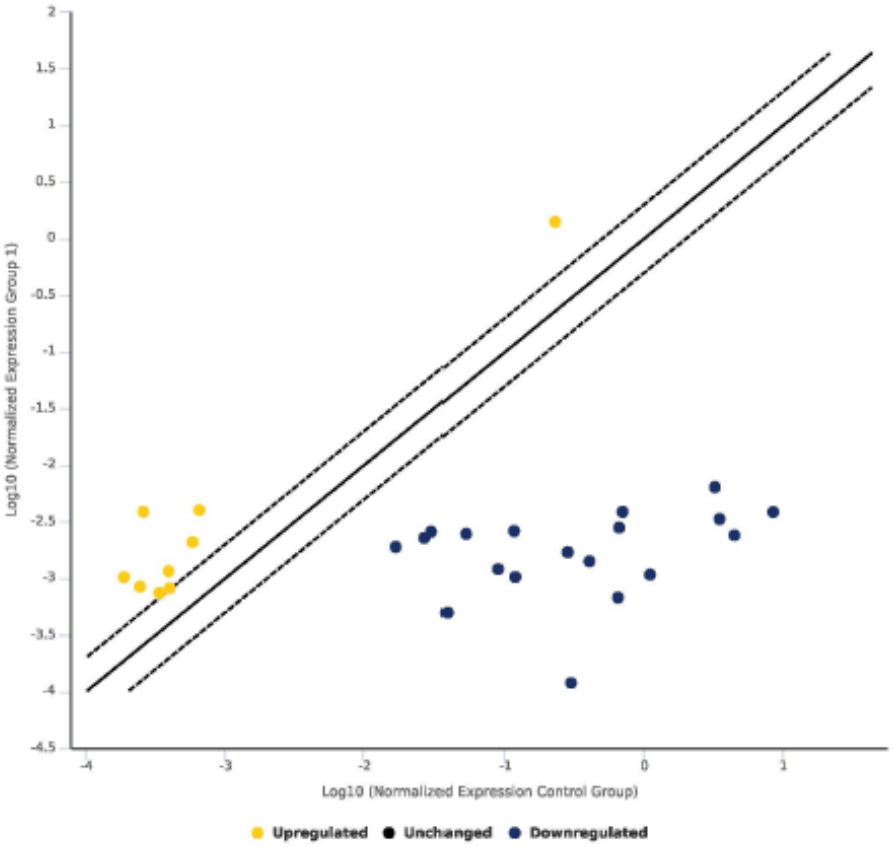

Figure 19. The scatter plot compares the normalized expression of the 28 differentially expressed bone ECM-associated genes on the PCR array between the scaffold and the polysterene group by plotting against one another. Symbols outside the dotted lines represent genes with at least a 2-fold expression difference between the respective tissues.

A significant downregulation was observed in the CS:Gel scaffold group in several genes encoding for ECM proteases, namely ADAM metallopeptidase with thrombospondin type 1 motif (ADAMTS1; FC=0.009), matrix metallopeptidase 2 (MMP2; FC=0.02), MMP14 (FC=0.09) TIMP metallopeptidase inhibitor 1 (TIMP1; FC=0.001) TIMP metallopeptidase inhibitor 2 (TIMP2; FC=0.006), TIMP metallopeptidase inhibitor 3 (TIMP3; FC=0.0035). Genes encoding for collagen type I, alpha 1 (COL1A1) chain and for collagen, type V, alpha 1 (COLVA1) chain were also downregulated in the scaffold group (FC=0.004 and FC=0.08, respectively). Furthermore, a reduced expression of the gene encoding for the secreted protein, acidic, cysteine-rich (SPARC, osteonectin) was observed in the scaffold group (FC=0.0019). Several other genes encoding ECM molecules were also decreased in the scaffold group, namely connective tissue growth factor (CTGF; FC=0.0005), c-

type lectin domain family 3, member B (CLEC3B; FC=0.013), extracellular matrix protein 1 (ECM1; FC=0.0123), fibronectin 1 (FN1; FC=0.0004), secreted phosphoprotein 1 (SPP1; FC=0.11), transforming growth factor beta-induced (TGFBI; FC=0.001), thrombospondin 1 and 2 (THBS1 and THBS2, respectively; FC=0.0009 and FC=0.047; respectively), tenascin C (TNC; FC=0.0055), versican (VCAN; FC=0.0004).

On the other hand a significant upregulation was observed in the CS:Gel scaffold group in genes encoding for ECM proteases, namely matrix metallopeptidase1 (MMP1; FC=5.4), MMP3 (FC=2.9), MMP9 (FC=14.8), MMP10 (FC=2), MMP11 (FC=6.1), MMP12 (FC=6.1), MMP13 (FC=2.2) and MMP16 (FC=3.6). The ECM vitronectin (VTN) was also found overexpressed in the CS:Gel scaffold group (VTN=3.41).

DISCUSSION

Natural biomaterials are being widely used as scaffolds in the field of tissue engineering due to their advantageous properties including porosity and pore size, biocompatibility and biodegradability, low cost and toxicity and capacity to support cell adhesion, viability and differentiation (35). Chitosan (CS) is a natural polycationic linear polysaccharide derived from partial deacetylation of chitin (21, 22) which possesses high biocompatibility, acceptable biodegradability, chemical similarity to the structure of extracellular matrix, anti-microbial activity and capacity to produce porous scaffolds and has thus been broadly studied as biomaterial for tissue-engineering applications (20, 21, 24, 36). In order to ameliorate the mechanical and biological properties of CS, the latter can be blended with gelatin (Gel), which demonstrates important properties for tissue engineering including such as biocompatibility, biodegradability, low antigenicity, high tensile strength and ability to promote cell adhesion, proliferation and differentiation (23, 37-39).

We have previously reported on the fabrication of natural low-cost 40:60% CS:Gel scaffold by chemical crosslinking with glutaraldehyde (GA) via the use of freeze drying (25). GA was used because of its ability to improve the mechanical properties of the scaffold and positively effect on the degradation rate (22), whereas the freeze drying method, was applied as it enables the formation of porous scaffolds with interconnecting pores (40). In addition, we have previously demonstrated that the aforementioned CS:Gel scaffolds promoted the survival and proliferation of BM-MSCs and had a positive effect on their osteogenic differentiation (25).

In view of these findings we have undertaken the present study aiming at extending our previous observations by gaining more insights into the effect of scaffolds on the synthesis and composition of bone ECM. To this end we comparatively characterized the composition of ECM produced by osteoblast differentiated BM-MSCs cultured on CS:Gel scaffolds or on tissue culture polystyrene (TCPS) by profiling the expression of 29 ECM-related genes via a commercially available PCR array. Moreover, we assessed by immunofluorescence the expression of representative ECM proteins (osteopontin, osteocalcin and collagen 1) by BM-MSCs seeded on scaffold or TCPS and differentiated towards osteoblasts.

In line with our previous report (25), in the present study CS:Gel scaffolds formed homogeneous interconnected spherical pores. Interestingly, the porosity and the open-pore structure are advantageous properties for the use of scaffolds in tissue engineering because they allow the ingrowth of cells, the diffusion of nutrients and play a critical role in cell adhesion and proliferation (37, 40). CS:Gel scaffolds actually contained the appropriate level of porosity and pore size as evidenced by the *in vitro* biological response of MSCs cultured on the composites. MSCs were isolated from the BM of healthy individuals and characterized as such by analyzing their morphological and immunophenotypic characteristics as well as their differentiation potential (29). 40%-60% CS:Gel scaffolds crosslinked with 0.1% GA promoted BM-MSC cell adhesion and proliferation. In fact, after 3 days of culture cells demonstrated the typical elongated fibroblast-like morphology of BM-MSCs. Cells had flattened, spread and completely covered the surface of the scaffold and formed inter-connections, consistent with tissue organization.

In the present study we also focused on the ability of the CS:Gel scaffolds to promote BM-MSC osteogenic differentiation. We thus assessed by real-time quantitate PCR analysis the expression of the osteogenic markers DLX5, RUNX2, ALP and OSC (41) in BM-MSCs cultured for 14 days on CS:Gel scaffolds, as compared to TCPS. The expression of DLX5 has not been previously studied in this scaffold. The mRNA expression of DLX5 and its downstream target RUNX2 (41, 42), which are the two master regulators of osteogenesis significantly increased in a time-dependent manner during BM-MSC osteogenic differentiation although with no statistically significant difference between GS-Gel and TCPS.

ALP and OSC are considered as markers of early and late osteoblastic differentiation, respectively (41). They are both implicated in bone mineralization, whereas the latter is also involved in bone ossification (41, 43). ALP and OSC gene expression demonstrated a time-dependent significant increase during osteogenic differentiation in both experimental groups. RUNX2 has been reported to regulate both ALP and OSC (42) and indeed the expression pattern of these two genes was consistent with that of RUNX2. Interestingly throughout osteogenic differentiation the expression of both ALP and OSC was significantly significantly upregulated in BM-

MSCs seeded on CS:Gel scaffolds, as compared to those seeded on TCPS, corroborating our previous findings (25).

As ALP and OSC are key components of bone ECM we assume that CS:Gel scaffolds promote the production of ECM by BM-MSCs undergoing osteogenic differentiation. ECM has a major impact in regard to bone tissue engineering as it mediates cell adhesion to biomaterials and its organization and production modulate the degree of cell attachment to the scaffolds. Within this context in the present study we were interested in getting a better understanding of the structure of the ECM produced by BM-MSCs undergoing osteoblastic differentiation on CS:Gel scaffolds. As the ECM production and structure have been shown to vary depending on the substrate cells are grown on, we evaluated the expression of 29 bone ECM-related genes via a commercially available PCR array comparatively in BM-MSCs induced to undergo osteogenic differentiation on scaffolds or TCPS. From a functional point of view these genes can be classified as encoding for collagens, ECM proteases, ECM protease inhibitors or other ECM constituents. In the next paragraphs we will critically discuss the results of the array and give a brief summary of the existing knowledge on the role in osteoblast differentiation and bone ECM formation of the 28/29 differentially expressed genes (in an alphabetical order).

ADAM metallopeptidase with thrombospondin type 1 motif, 1 (ADAMTS1) mRNA expression has been identified by RT-PCR in cultures of rat osteoblasts treated with ascorbic acid, beta-glycerophosphate and dexamethasone (44). ADAMTS1 expression has been reported to follow the expression of osteocalcin during in vitro mineralization. We found that BM-MSCs induced to undergo osteogenic differentiation on CS:Gel scaffolds, demonstrate a reduced expression of ADMATS1 as compared to BM-MSCs differentiated on TCPS, even though the expression of osteocalcin was significantly increased in the former group. Given that in the present study the expression of all evaluated genes in BM-MSCs differentiated on scaffolds was consistently low, any comparison with the TCPS needs particular caution.

C-type lectin domain family 3, member B (CLEC3B) is an ECM protein which is expressed by cultured osteoblastic cells in vitro in parallel with mineralization, in a pattern similar to that of bone sialoprotein, one of the late bone differentiation

markers (45). In vivo, CLC3B promotes bone formation (45). We have demonstrated that CLEC3B is downregulated in BM-MSCs undergoing osteogenic differentiation on the CS:Gel scaffolds. The impact of this downregulation in the ECM produced by MSCs on the scaffolds is currently unknown.

Collagens comprise a large family of multimeric proteins with up to 38 genes giving rise to 20 different collagens (46, 47). After these large polypeptide chains are synthesized, they become intertwined with two other chains in a triple helical structure. The major collagen triplex in bone matrix is type I that is composed of two a1 chains (also called COL1A1) and one a2 chain (COL2A1) (46, 47). Other types of collagen, such as types III and V, are also present at low levels in bone and appear to modulate the fibril diameter(46, 47). Accumulating evidence suggests that collagen type I has direct effects on important bone cell functions including apoptosis, cell proliferation and differentiation (47). Its main function though is to serve as template for matrix deposition and mineralization and to bind and orient other proteins that nucleate hydroxyapatite deposition (46, 47). Our findings demonstrate a significant downregulation of the components of collagen type I and collagen type V, namely collagen 1A1 and collagen VA1, respectively, in BM-MSCs undergoing osteogenic differentiation. In view of the documented osteogenesis promoting role of the scaffold, these findings require further investigation.

Connective tissue growth factor (CTGF) is a cysteine rich, ECM protein which is produced and secreted by osteoblasts in vitro (48). CTGF has been shown to stimulate osteoblast proliferation and differentiation as well as matrix production. CTGF levels in osteoblasts are induced by TGFβ1(48). In our experimental setting TGFβ1 is down-regulated in BM-MSCs induced to undergo osteogenic differentiation on CS:Gel scaffolds and this might account, at least in part for the reduced expression of CTGF in these cells.

Extracellular matrix protein 1 (ECM1) is a secreted glycoprotein that has been suggested to act as a negative regulator of endochondral bone formation, by inhibiting ALP and bone mineralization (49, 50). In our study ECM1 was found to be significantly downregulated in BM-MSCs undergoing osteogenic differentiation on

CS:Gel scaffolds. This finding may be associated with the increased ALP expression in the scaffold group.

Fibronectin 1 (FN1) is one of the most abundant glycoproteins in bone ECM, which is produced by osteoblasts (47). It contains a short amino acid sequence (Arg-Gly-Asp or RGD) that is critical for binding to integrin receptors located at the osteoblast surface and for subsequent osteoblast differentiation and survival(47). Furthermore FN1 is needed for the polymerization of collagen type I and has therefore been suggested to play a key role in bone matrix formation and integrity(46). According to our findings FN1 is significantly downregulated in BM-MSCs undergoing osteogenic differentiation on scaffolds. How this downregulation affects ECM produced by BM-MSCs differentiated on scaffolds is currently unknown.

Matrix metalloproteinases (MMPs) are the major protease family responsible for the cleavage of the ECM proteins as well as proteins unrelated to the ECM (51). MMPs mediate ECM remodeling, in association with tissue-specific and cell-anchored inhibitors (TIMPs and RECK, respectively) (51). In bone tissue many MMPs and their inhibitors have been identified thus far. They are implicated in osteoblast/osteocyte differentiation, bone formation, bone resorption and also in osteoblast recruitment and migration during bone remodeling (52). Osteoblasts are the main source of MMPs in bone, namely MMP1, MMP2, MMP3, MMP8, MMP9, MMP10, MMP11, MMP12, MMP13, MMP14, and MMP16 (51, 52). In the present study we found that 10 MMPs are differentially expressed in BM-MSCs undergoing osteogenic differentiation on CS:Gel scaffolds as compared to TCPS. More precisely, MMP2, and MMP14 were downregulated, whereas MMP1, MMP3, MMP9, MMP10, MMP11, MMP12, MMP13 and MMP16 were up-regulated. MMP16 controls cell viability. MMP-2 is important for differentiation and survival; MMP14 is crucial for osteoblast survival during osteoblast/osteocyte transition (51, 52). Furthermore, MMP2, MMP13, and MMP14 are required for adequate lacunae formation in osteocytes. Interestingly, MMP16 has been shown to compensate for the action of MMP14 (52). We thus hypothesize that the over-expression of MMP16 in BM-MSCs undergoing osteogenic differentiation on CS:Gel scaffolds may counteract in terms of

biological effect the down-regulation of MMP14, thereby resulting in promotion of osteogenesis by the scaffolds.

Secreted protein, acidic, cysteine-rich (SPARC, osteonectin) (46, 53) is the most abundant noncollagenous glycoprotein in bone, that can bind to both collagen fibrils and hydroxyapatite. SPARC is expressed by osteoblasts undergoing active matrix deposition. Its concentration in bone matrix is variable and appears to be inversely correlated with the degree of calcification. It promotes osteoblast differentiation and cell survival similar to other ECM proteins (46, 53). SPARC expression was down-regulated in BM-MSCs undergoing osteogenic differentiation on CS:Gel scaffolds; it would be interesting to investigate how SPARC underexpression affects the formation and function of bone matrix produced BM-MSCs differentiated on scaffolds.

Secreted phosphoprotein 1 (SPP1, osteopontin), is a secreted glycoprotein with the characteristics of a matricellular protein. It is produced by osteoblasts and, to a lesser extent, by osteocytes, making it a late marker of osteoblastic differentiation and an early marker of matrix mineralization (46). SPP1 is involved in several biological processes, including biomineralization, cell attachment and cell signaling (46). Notably, phosphorylated SPP1 inhibits mineralization in vitro and in vivo, but the dephosphorylated form does not have this effect. Furthermore, in vivo studies suggest that SPP1 is a potent regulator of osteoclast activity (46). Our findings indicate a significant down-regulation of SPP1 in BM-MSCs undergoing osteogenic differentiation on CS:Gel scaffolds. It would be interesting to investigate how SPP1 underexpression affects the formation and function of bone matrix produced BM-MSCs differentiated on scaffolds.

Transforming growth factor, beta-induced (TGFBI) is an extracellular ECM protein binds to integrins and other ECM proteins to mediate cell adhesion and migration. A few in vitro studies related to bone metabolism have found that TGFBI has a positive effect on the adhesion and migration of osteoblasts and a negative effect on their differentiation and mineralization. Our findings demonstrate that TGFBI is significantly downregulated in BM-MSCs induced to undergo osteogenic

differentiation on CS:Gel scaffolds as compared to those on TCP. This observation corroborates the osteogenesis promoting role of the scaffolds.

Tenascin C (TNC) is an ECM glycoprotein synthesized by osteoblasts (54). In vitro studies have demonstrated that TNC increases during osteoblast differentiation and that it exerts a positive effect on ALP expression and osteoblast mineralization (54). In the present study we have shown that TNC is down-regulated in BM-MSCs undergoing osteogenic differentiation on CS:Gel scaffolds. This observation contradicts the already documented osteogenesis promoting capacity of the CS:Gel scaffold and ALP overexpression and requires additional validation.

Thrombospondins 1 and 2 are complex, multi-functional non-collagenous ECM proteins (55). According to our findings they are down-regulated in BM-MSCs undergoing osteogenic differentiation on CS:Gel scaffolds. As thrombospondin 1 has been reported to inhibit MSC osteogenic differentiation and mineralization(56) its decreased expression might be anticipated in view of the osteogenesis supporting role of the scaffolds.

TIMP metallopeptidase inhibitors are a multifunctional protein family originally characterized as able to inhibit the catalytic activity of all MMPs in the ECM (51). Classically, TIMP1 is known to have high affinity for MMP9, medium affinity for MMP3 and MMP13, and a low ability to inhibit MMP2, MMP14 and MMP16. TIMP-2 has high affinity for MMP2 and acts as an inhibitor at high concentrations or participates in the activation of pro-MMP2 when in low concentrations. TIMP-3 displays high affinity for MMP1, MMP2 and MMP14. There is evidence suggesting that specific gene down or upregulation of MMP/TIMP is important for osteoblast/osteocyte transition and matrix mineralization. In the present study we observed a downregulation of TIMP-1, TIMP-2 and TIMP-3 in the scaffold group. On the other hand MMP1, MMP3, MMP9, MMP10, MMP11, MMP12 and MMP13 are found upregulated in the scaffold group as previously discussed. How the imbalance between MMP and TIMP affects the biology of ECM produced by BM-MSCs undergoing osteogenic differentiation on scaffolds is currently and warrants further investigation.

Versican (VCAN) is another proteoglycan related to aggrecan (46). In rats VCAN has been shown to increase in osteogenesis, yet its function in bone is largely unknown (46). In the present study we have shown that VCAN is significantly reduced in BM-MSCs undergoing osteogenic differentiation on CS:Gel scaffolds. The biological significance of this finding is unknown and it certainly needs to be confirmed in additional studies.

Vitronectin (VTN) expression was significantly up-regulated in BM-MSCs undergoing osteogenic differentiation on CS:Gel scaffolds as compared to TCPS. This adhesive protein contains the Arg-Gly-Asp (RGD) domain recognized by the cells via integrin receptors. VTN is anchored to the ECM via collagen binding and has been shown to promote bone cell adhesion as well as the osteogenic differentiation of MSCs in vitro (57, 58).

Taken together and bearing in mind the aforementioned limitations in interpreting the differential expression of the bone ECM-associated genes between the two experimental groups, in the scaffold group a significant downregulation of collagens, ECM protease inhibitors and various other ECM molecules was observed. On the other hand ECM proteases (MMPs) as well as VTN were increased. How this differential expression in 28 out of 29 evaluated genes affects the formation, deposition and function of ECM produced by BM-MSCs undergoing osteogenesis on CS:Gel scaffolds and how this will eventually impact on cell survival, proliferation differentiation and mineralization requires further investigation.

In the present study we also assessed at the protein level the expression of molecules associated with bone ECM, namely osteopontin, osteocalcin and collagen type I using immunofluorescence in BM-MSCs undergoing osteogenic differentiation on TCPS or on CS:Gel scaffolds. The protein expression corroborates the PCR array results since a more intense expression of collagen type I A1 and osteopontin was seen in TCPS compared to CS:Gel scaffold. However, the staining methods are different and any comparison might be inaccurate. Anyhow, the findings of the collagen type I A1 and osteopontin protein expression provides additional evidence that our CS-Gel scaffold supports osteogenesis. On the other hand, in accordance with previously reported data recognizing osteocalcin protein as a late marker of

osteogenic differentiation, we identified low levels of this protein in both CS:Gel scaffolds and TCPS (25).

In conclusion, in the current study we have extended our previous work (25) regarding the osteogenesis supporting capacity of 40:60% CS:Gel scaffolds by comparatively evaluating the composition of ECM produced by BM-MSCs induced to undergo osteogenic differentiation on the scaffolds or on TCPS. To this end, BM-MSCs were isolated from healthy individuals and following their appropriate characterization they were cultured on CS:Gel scaffolds, which were fabricated by chemical crosslinking with GA via the use of freeze drying. Osteogenic differentiation was subsequently induced and the osteogenesis promoting capacity of the scaffolds was confirmed by mRNA expression of early and late osteogenic markers, further validating our previous results (25). Furthermore, we evaluated the collagen type I A1, osteopontin and osteocalcin protein expression by immunofluorescence providing additional evidence that CS-Gel scaffold supports osteogenesis. We then assessed the mRNA expression of 29 genes associated with bone ECM in BM-MSCs induced to differentiate on scaffolds or polystyrene. 28/29 genes functionally classified as encoding for collagens, ECM proteases, ECM protease inhibitors and other ECM molecules were differentially expressed between the two experimental groups. To the best of our knowledge this is the first study reporting on a comprehensive characterization of the bone ECM produced by BM-MSCs induced to differentiate on CS:Gel scaffolds. Our findings will be further validated and expanded including a biomechanical analysis of long-term cultured constructs to better clarify the complex cell-scaffold interactions which are important for bone tissue engineering applications.

REFERENCES

1. Amini AR, Laurencin CT, Nukavarapu SP. Bone tissue engineering: recent advances and challenges. Critical reviews in biomedical engineering. 2012;40(5):363-408.
2. Florencio-Silva R, Sasso GR, Sasso-Cerri E, Simoes MJ, Cerri PS. Biology of Bone Tissue: Structure, Function, and Factors That Influence Bone Cells. Biomed Res Int. 2015;2015:421746.
3. Sila-Asna M, Bunyaratvej A, Maeda S, Kitaguchi H, Bunyaratavej N. Osteoblast differentiation and bone formation gene expression in strontium-inducing bone marrow mesenchymal stem cell. The Kobe journal of medical sciences. 2007;53(1-2):25-35.
4. Capulli M, Paone R, Rucci N. Osteoblast and osteocyte: games without frontiers. Archives of biochemistry and biophysics. 2014;561:3-12.
5. Fakhry M, Hamade E, Badran B, Buchet R, Magne D. Molecular mechanisms of mesenchymal stem cell differentiation towards osteoblasts. World journal of stem cells. 2013;5(4):136-48.
6. Matic I, Cocco S, Ferraina C, Martin-Jimenez R, Florenzano F, Crosby J, et al. Neuroprotective coordination of cell mitophagy by the ATPase Inhibitory Factor 1. Pharmacological research. 2016;103:56-68.
7. Rochefort GY, Pallu S, Benhamou CL. Osteocyte: the unrecognized side of bone tissue. Osteoporosis international : a journal established as result of cooperation between the European Foundation for Osteoporosis and the National Osteoporosis Foundation of the USA. 2010;21(9):1457-69.
8. Schaffler MB, Cheung WY, Majeska R, Kennedy O. Osteocytes: master orchestrators of bone. Calcified tissue international. 2014;94(1):5-24.
9. Raggatt LJ, Partridge NC. Cellular and molecular mechanisms of bone remodeling. The Journal of biological chemistry. 2010;285(33):25103-8.
10. Rucci N. Molecular biology of bone remodelling. Clinical cases in mineral and bone metabolism : the official journal of the Italian Society of Osteoporosis, Mineral Metabolism, and Skeletal Diseases. 2008;5(1):49-56.
11. Buckwalter JA, Glimcher MJ, Cooper RR, Recker R. Bone biology. I: Structure, blood supply, cells, matrix, and mineralization. Instructional course lectures. 1996;45:371-86.
12. Ma J, Both SK, Yang F, Cui FZ, Pan J, Meijer GJ, et al. Concise review: cell-based strategies in bone tissue engineering and regenerative medicine. Stem Cells Transl Med. 2014;3(1):98-107.
13. Colnot C. Cell sources for bone tissue engineering: insights from basic science. Tissue engineering Part B, Reviews. 2011;17(6):449-57.
14. Pontikoglou C, Deschaseaux F, Sensebe L, Papadaki HA. Bone marrow mesenchymal stem cells: biological properties and their role in hematopoiesis and hematopoietic stem cell transplantation. Stem cell reviews. 2011;7(3):569-89.
15. Berger J, Reist M, Mayer JM, Felt O, Peppas NA, Gurny R. Structure and interactions in covalently and ionically crosslinked chitosan hydrogels for biomedical applications. European journal of pharmaceutics and biopharmaceutics : official journal of Arbeitsgemeinschaft fur Pharmazeutische Verfahrenstechnik eV. 2004;57(1):19-34.
16. Szczepanska J, Pawlowska E, Synowiec E, Czarny P, Rekas M, Blasiak J, et al. Protective effect of chitosan oligosaccharide lactate against DNA double-strand breaks induced by a model methacrylate dental adhesive. Medical science monitor : international medical journal of experimental and clinical research. 2011;17(8):BR201-8.
17. O'Brien FJ, Harley BA, Yannas IV, Gibson LJ. The effect of pore size on cell adhesion in collagen-GAG scaffolds. Biomaterials. 2005;26(4):433-41.
18. Polo-Corrales L, Latorre-Esteves M, Ramirez-Vick JE. Scaffold design for bone regeneration. J Nanosci Nanotechnol. 2014;14(1):15-56.

19. Burg KJ, Porter S, Kellam JF. Biomaterial developments for bone tissue engineering. Biomaterials. 2000;21(23):2347-59.
20. Ahmed S, Annu, Ali A, Sheikh J. A review on chitosan centred scaffolds and their applications in tissue engineering. International journal of biological macromolecules. 2018;116:849-62.
21. Di MA, Sittinger M, Risbud MV. Chitosan: a versatile biopolymer for orthopaedic tissue-engineering. Biomaterials. 2005;26(30):5983-90.
22. Huang Y, Onyeri S, Siewe M, Moshfeghian A, Madihally SV. In vitro characterization of chitosan-gelatin scaffolds for tissue engineering. Biomaterials. 2005;26(36):7616-27.
23. Djagny VB, Wang Z, Xu S. Gelatin: a valuable protein for food and pharmaceutical industries: review. Critical reviews in food science and nutrition. 2001;41(6):481-92.
24. Miranda SC, Silva GA, Hell RC, Martins MD, Alves JB, Goes AM. Three-dimensional culture of rat BMMSCs in a porous chitosan-gelatin scaffold: A promising association for bone tissue engineering in oral reconstruction. Archives of oral biology. 2011;56(1):1-15.
25. Georgopoulou A, Papadogiannis F, Batsali A, Marakis J, Alpantaki K, Eliopoulos AG, et al. Chitosan/gelatin scaffolds support bone regeneration. J Mater Sci Mater Med. 2018;29(5):59.
26. Autissier A, Le Visage C, Pouzet C, Chaubet F, Letourneur D. Fabrication of porous polysaccharide-based scaffolds using a combined freeze-drying/cross-linking process. Acta biomaterialia. 2010;6(9):3640-8.
27. Martins AM, Alves CM, Reis RL, Mikos AG, Kasper FK. Toward osteogenic differentiation of marrow stromal cells and in vitro production of mineralized extracellular matrix onto natural scaffolds. Biological Interactions on Materials Surfaces: Springer; 2009. p. 263-81.
28. Kastrinaki MC, Sidiropoulos P, Roche S, Ringe J, Lehmann S, Kritikos H, et al. Functional, molecular and proteomic characterisation of bone marrow mesenchymal stem cells in rheumatoid arthritis. AnnRheumDis. 2008;67(6):741-9.
29. Dominici M, Le Blanc K, Mueller I, Slaper-Cortenbach I, Marini F, Krause D, et al. Minimal criteria for defining multipotent mesenchymal stromal cells. The International Society for Cellular Therapy position statement. Cytotherapy. 2006;8(4):315-7.
30. Chatzinikolaidou M, Pontikoglou C, Terzaki K, Kaliva M, Kalyva A, Papadaki E, et al. Recombinant human bone morphogenetic protein 2 (rhBMP-2) immobilized on laser-fabricated 3D scaffolds enhance osteogenesis. Colloids SurfB Biointerfaces. 2017;149:233-42.
31. Delorme B, Charbord P. Culture and characterization of human bone marrow mesenchymal stem cells. Methods MolMed. 2007;140:67-81.
32. Cartmell GRKaSH. Genes and Proteins Involved in the Regulation of Osteogenesis 2007.
33. Pavlaki K, Pontikoglou CG, Demetriadou A, Batsali AK, Damianaki A, Simantirakis E, et al. Impaired proliferative potential of bone marrow mesenchymal stromal cells in patients with myelodysplastic syndromes is associated with abnormal WNT signaling pathway. Stem cells and development. 2014;23(14):1568-81.
34. Batsali AK, Pontikoglou C, Koutroulakis D, Pavlaki KI, Damianaki A, Mavroudi I, et al. Differential expression of cell cycle and WNT pathway-related genes accounts for differences in the growth and differentiation potential of Wharton's jelly and bone marrow-derived mesenchymal stem cells. Stem cell research & therapy. 2017;8(1):102.
35. Ma PX. Biomimetic materials for tissue engineering. AdvDrug DelivRev. 2008;60(2):184-98.
36. Cheung RC, Ng TB, Wong JH, Chen Y, Chan WY. Marine natural products with anti-inflammatory activity. Applied microbiology and biotechnology. 2016;100(4):1645-66.

37. Lawrence BJ, Madihally SV. Cell colonization in degradable 3D porous matrices. Cell adhesion & migration. 2008;2(1):9-16.
38. Santoro M, Tatara AM, Mikos AG. Gelatin carriers for drug and cell delivery in tissue engineering. Journal of controlled release : official journal of the Controlled Release Society. 2014;190:210-8.
39. Thein-Han WW, Saikhun J, Pholpramoo C, Misra RD, Kitiyanant Y. Chitosan-gelatin scaffolds for tissue engineering: physico-chemical properties and biological response of buffalo embryonic stem cells and transfectant of GFP-buffalo embryonic stem cells. Acta biomaterialia. 2009;5(9):3453-66.
40. Mao JS, Zhao LG, Yin YJ, Yao KD. Structure and properties of bilayer chitosan-gelatin scaffolds. Biomaterials. 2003;24(6):1067-74.
41. Kirkham Gr CS. Genes and Proteins Involved in the Regulation of Osteogenesis. In: Ashammakhi N RR, Chiellini E, editor. Topics in Tissue Engineering,. 32007.
42. Liu TM, Lee EH. Transcriptional regulatory cascades in Runx2-dependent bone development. Tissue engineering Part B, Reviews. 2013;19(3):254-63.
43. Franceschi RT. The developmental control of osteoblast-specific gene expression: role of specific transcription factors and the extracellular matrix environment. Critical reviews in oral biology and medicine : an official publication of the American Association of Oral Biologists. 1999;10(1):40-57.
44. Lind T, McKie N, Wendel M, Racey SN, Birch MA. The hyalectan degrading ADAMTS-1 enzyme is expressed by osteoblasts and up-regulated at regions of new bone formation. Bone. 2005;36(3):408-17.
45. Wewer UM, Ibaraki K, Schjorring P, Durkin ME, Young MF, Albrechtsen R. A potential role for tetranectin in mineralization during osteogenesis. The Journal of cell biology. 1994;127(6 Pt 1):1767-75.
46. Boskey AL RP. The Regulatory Role of Matrix Proteins in Mineralization of Bone. Osteoporosis2013. p. 235-55.
47. Young MF. Bone matrix proteins: their function, regulation, and relationship to osteoporosis. Osteoporosis international : a journal established as result of cooperation between the European Foundation for Osteoporosis and the National Osteoporosis Foundation of the USA. 2003;14 Suppl 3:S35-42.
48. Arnott JA, Lambi AG, Mundy C, Hendesi H, Pixley RA, Owen TA, et al. The role of connective tissue growth factor (CTGF/CCN2) in skeletogenesis. Critical reviews in eukaryotic gene expression. 2011;21(1):43-69.
49. Deckers MM, Smits P, Karperien M, Ni J, Tylzanowski P, Feng P, et al. Recombinant human extracellular matrix protein 1 inhibits alkaline phosphatase activity and mineralization of mouse embryonic metatarsals in vitro. Bone. 2001;28(1):14-20.
50. Gentili C, Cancedda R. Cartilage and bone extracellular matrix. Current pharmaceutical design. 2009;15(12):1334-48.
51. Paiva KBS, Granjeiro JM. Matrix Metalloproteinases in Bone Resorption, Remodeling, and Repair. Progress in molecular biology and translational science. 2017;148:203-303.
52. Liang HPH XJ, Xue M, Jackson CJ. Matrix metalloproteinases in bone development and pathology: current knowledge and potential clinical utility. Metalloproteinases In Medicine. 2016;3:93-102.
53. Rosset EM, Bradshaw AD. SPARC/osteonectin in mineralized tissue. Matrix biology : journal of the International Society for Matrix Biology. 2016;52-54:78-87.
54. Li C, Cui Y, Luan J, Zhou X, Li H, Wang H, et al. Tenascin C affects mineralization of SaOS2 osteoblast-like cells through matrix vesicles. Drug discoveries & therapeutics. 2016;10(2):82-7.
55. Alford AI, Hankenson KD. Matricellular proteins: Extracellular modulators of bone development, remodeling, and regeneration. Bone. 2006;38(6):749-57.

56. Amend SR, Uluckan O, Hurchla M, Leib D, Novack DV, Silva M, et al. Thrombospondin-1 regulates bone homeostasis through effects on bone matrix integrity and nitric oxide signaling in osteoclasts. Journal of bone and mineral research : the official journal of the American Society for Bone and Mineral Research. 2015;30(1):106-15.
57. Salasznyk RM, Williams WA, Boskey A, Batorsky A, Plopper GE. Adhesion to Vitronectin and Collagen I Promotes Osteogenic Differentiation of Human Mesenchymal Stem Cells. Journal of biomedicine & biotechnology. 2004;2004(1):24-34.
58. Hidalgo-Bastida LA, Cartmell SH. Mesenchymal stem cells, osteoblasts and extracellular matrix proteins: enhancing cell adhesion and differentiation for bone tissue engineering. Tissue engineering Part B, Reviews. 2010;16(4):405-12.